Regional and seasonal variability in the vertical distribution of mesozooplankton in the Greenland Sea

Claudio Richter

Ber. Polarforsch. 154 (1994)
ISSN 0176 - 5027

Summary

A large-scale regional and seasonal zooplankton investigation was carried out in the Greenland Sea covering the entire water column down to 3000 m depth. It focussed on the composition and vertical distribution of zooplankton in relation to the hydrographic régime (i) and in course of time (ii). Sampling was carried out with vertical Multinet hauls (150 µm mesh) in nine depth strata: 3000 (or sea floor)-2000-1500-1000-500-400-300-200-100-0 m.

(i) The regional study comprised a transect along 75°N in November 1988, occupying one station in the Atlantic domain of the West Spitsbergen Current (WSC) and three stations in the arctic domain of the Greenland Sea Gyre (GSG). The WSC station showed a low number of individuals and species and a relatively even distribution of individuals among species. *Calanus finmarchicus* (Calanoida, Copepoda) dominated in abundance (40%) and biomass (55%). Within the GSG, *Oithona* (Cyclopoida, Copepoda) was numerically dominant (38%-58%) and *Calanus hyperboreus* in terms of biomass (35%). Biomass varied only little along the transect (13±1 g DW$*$m^{-2}). Highest numbers of individuals were found in the upper 500 m, while a large fraction of the biomass was located below.

(ii) The seasonal study encompassed six stations in the GSG, revisited in late fall, winter, early and late summer of 1988/89 and spring of 1993. Species composition remained fairly constant throughout the investigation period, around 48 species, with *Oithona* dominating in abundance (53%) and *C. hyperboreus* in biomass (32%). Integrated abundance varied by a factor of 2.5, with maximum values in June ($7.4*10^5$ n$*$m^{-2}). Integrated biomass was high (14 g DW m^{-2}) and remarkably constant, varying by a factor of 1.5 between the winter minimum and the late summer maximum.

Abundance was maximal at the surface throughout the light season, whereas the biomass maximum occurred only briefly at the surface in early summer and prevailed in the subsurface for most of the year.

Depth was the main factor shaping the community, revealing distinct assemblages of

(1) widely distributed and abundant species *(Oithona* spp., *Oncaea* spp., *Calanus* spp., *Pseudocalanus minutus)*

(2) mesopelagic resident species of restricted range (Aetideidae, Ostracoda, Chaetognatha) and

(3) bathypelagic resident species of restricted range (Cnidaria).

Distribution patterns of (1) and (2) were highlighted and discussed with regard to potential food requirements and storage capacities (body size). Seasonal vertical migrations were marked for herbivorous calanoid copepods. Their extent and timing appeared to be related to body size, both inter- and intraspecifically. *Calanus hyperboreus* carried out extensive vertical migrations exceeding 1500 m with a brief surface period for the larger stages. The smaller *Pseudocalanus minutus* remained longer at the surface hibernating at intermediate depths. *Calanus finmarchicus* performed shallower seasonal migrations, but no pattern was obvious for the omnivorous *Metridia longa.* The ubiquitous cyclopoid copepods occurred in high numbers throughout the year, with *Oithona* occupying the epi- and *Oncaea* the meso- and bathypelagial, both reproducing at the surface in early summer.

A rich mesopelagic community of omni- and carnivorous copepods, ostracods and chaetognaths was encountered, showing a seasonally stable vertical partitioning of the water column. It is estimated that a considerable portion of the secondary production goes into the mesopelagic food web, while the bathypelagic zone might serve as a refuge for overwintering herbivore stocks. High overall biomass and low seasonal variability characterize the Greenland Sea Gyre as a remarkably stable system, in spite of marked seasonal variations in food availability.

1 Introduction

Little is known of the plankton fauna of the central Greenland Sea, let alone its quantitative composition and vertical distribution. Seasonal investigations including the deep sea are limited to the detailed investigations carried out on the weather ships of the station 'M' in the Norwegian Sea (66°N, 2°E), where regular plankton collections were made from 1948 to 1951 down to 2000 m (Wiborg 1954, Østvedt 1955). Less systematic investigations were conducted on the numerous drifting ice islands (T3, Arlis II, NP-22, NP-23) in the Arctic Ocean to a maximum depth of 3000 m (Hopkins 1969, Kosobokova 1982). Comparable investigations down to 2000-3000 m from other high latitude oceanic regions are restricted to the Bering Sea (Vinogradov 1970), the station 'P' in the North Pacific (McAllister 1961), the Subantarctic and Antarctic (Foxton 1956).

The present study thus fills a geographic gap between the investigations carried out in the polar (ice islands) and Atlantic (weather ship 'M') domains of the Arctic-Atlantic continuum. The Greenland Sea Project (GSP), a joint oceanographic research program of eleven nations investigating the processes of water mass transformation and transport in the Greenland Sea (GSP Group 1990), offered a unique possibility for biologists to collect samples at all seasons and to combine their results with a good hydrographical data set. Based on the available zooplankton material from the 1988/89 field phase of the GSP, which was supplemented with a station occupied in spring 1993, the present investigation addresses the large-scale vertical distribution of mesozooplankton in the Greenland Sea. It identifies the main contributors to abundance and biomass and follows their seasonal and regional changes over the entire water column down to 3000 m. Adverse meteorological conditions and logistical constraints limited the number of observations to a minimum: Repeated sampling at all seasons at one central station in the Greenland Sea Gyre and a zonal transect of four stations across the Greenland Sea in late fall. However, the resulting data set is exceptional in covering all seasons in this remote ocean area and in spanning the entire vertical range down to the deep sea.

Previous investigations in the Fram Strait and Nansen Basin mostly were restricted to the upper 500 m. They had already indicated that a potentially large fraction of the ostracod and chaetognath community was likely to be missed below (Haberstroh 1985, Mumm 1991). Late-summer investigations from the Greenland Sea (cf. Smith and Schnack-Schiel 1990) as well as Østvedt's (1955) seasonal study in the Norwegian Sea left little doubt that the main biomass carriers, *Calanus* spp. descended beyond this horizon to overwinter. Hirche (1991) was the first to show that the fall descent of *Calanus* spp. in the Greenland Sea exceeded 1000 m, while in the Arctic Ocean the bulk of the wintering population remained within the upper 500 m (Dawson 1978, Rudyakov 1983). The present study extends Hirche's (1991) observations to the whole zooplankton community over all seasons, highlighting the following questions:

- What is the species composition, abundance and biomass in this high latitude oceanic system? How does it vary in the course of time?
- What are the main factors shaping the zooplankton communities?
- Which are the dominant taxa and how does their distribution vary with depth and time?
- What are their life cycles and how are they geared to the seasonal production cycle?
- Are there general conclusions to be drawn? E.g.
  - between the distribution patterns of herbivores, omnivores and carnivores?

- between different sizes? Does size-dependent storage capacity affect the timing and magnitude of the seasonal vertical migrations?

On the basis of the vertically almost homogenous water column (Budéus et al. 1993) and the very low horizontal current velocities in the Greenland Sea Gyre (Visbeck 1993) it was assumed that biological changes outweigh physical variability within the gyre. The large-scale cyclonic circulation (e.g. Swift 1986) was further assumed to retain the plankton in the area assuring repeated sampling of essentially the same population over time. To assess the effect of circulation and water masses on the vertical distribution and quantitative composition of the zooplankton a regional transect was carried out across the Atlantic and arctic[1] domains of the Greenland Sea in late fall 1988.

Overall results are compared with other high latitude ocean areas. Species numbers and diversity are discussed with respect to hydrography and selection of cold-adapted species (Vinogradov 1970), biomass with respect to circulation and the seasonal production cycle and the vertical transport of biomass. Its level and variability is considered an indicator for efficient resource-partitioning in this highly food-limited system (Smith and Sakshaug 1990).

The investigation is a contribution to ongoing and planned research in the area, namely the international Greenland Sea Project (GSP), the joint research project at Kiel University (SFB 313) and MARE COGNITUM/GLOBEC (Norway).

[1] minuscule/majuscule notation adopted from Swift (1986)

2 Study area

The Greenland Sea can be delimited by hydrographical and topographical features, for bottom topography strongly affects the circulation and the distribution of water masses in the Nordic Seas (Johannessen 1986).

Bathymetry

Surrounded by the Arctic Ocean, the Barents, Norwegian and Iceland Seas, the Greenland Sea is bounded by the Fram Strait in the north, Spitsbergen and the Barents Sea slope in the east, Mohns ridge in the southeast, the Jan Mayen fracture zone in the south, and the Greenland coast in the west (Fig. 2.1). According to bathymetry, the Greenland Sea can be further divided into a shelf area and two deep basins. The east Greenland shelf is narrow in the south (50 km), but progressively broadens towards the north. It reaches halfway through the Fram Strait at its maximum zonal extension (280 km, Perry 1986), breaking away rather precipitously into the abyssal plains of the Greenland Sea. The Greenland fracture zone separates the larger and deeper (3400-3600 m) Greenland Basin from the Boreas Basin (3200 m) to the north. The mid-ocean ridge demarcates the southern and eastern borders of these basins along Mohns and Knipovich ridge. Anchored above these bottom features are hydrographic fronts which separate water masses of widely disparate origin, indicating strong topographic steering of the wind-driven current system (Quadfasel and Meincke 1987, van Aken et al. 1991).

Circulation

The most conspicuous feature of the Greenland Sea circulation is the meridional flow of two opposing boundary currents. They carry large amounts of heat and salt from the North Atlantic into high latitudes along the eastern side, and ice and fresh water from the Arctic Ocean towards lower latitudes along the western side (Fig. 2.1). Zonal branching of this meridional flow occurs along topographic barriers and gives rise to a counter-clockwise circulation pattern in the Greenland Sea. Thus, an eastward deflection of part of the southbound East Greenland Current (EGC) occurs along the Jan Mayen fracture zone, known as the Jan Mayen Current. The westward deflection of part of the West Spitsbergen Current (WSC) has been found associated with the Molloy seamounts and the Hovgaard fracture zone in the Fram Strait (Quadfasel et al. 1987). The latter recirculating branches are termed Return Atlantic Current (RAC). Owing to the topographic steering of the mainly barotropic flow, cyclonic gyres are formed over each of the subbasins (Quadfasel and Meincke 1987, not shown in Figure 2.1).

Water masses

Swift (1986) distinguishes the Atlantic and polar domains of the Greenland Sea periphery from the „arctic waters" of the central basins (Helland-Hansen and Nansen 1909). These domains are separated by meridional hydrographic fronts: the East Greenland Polar Front (EGPF) to the west and the Arctic Front to the east. Swift (1986) points to the fact that

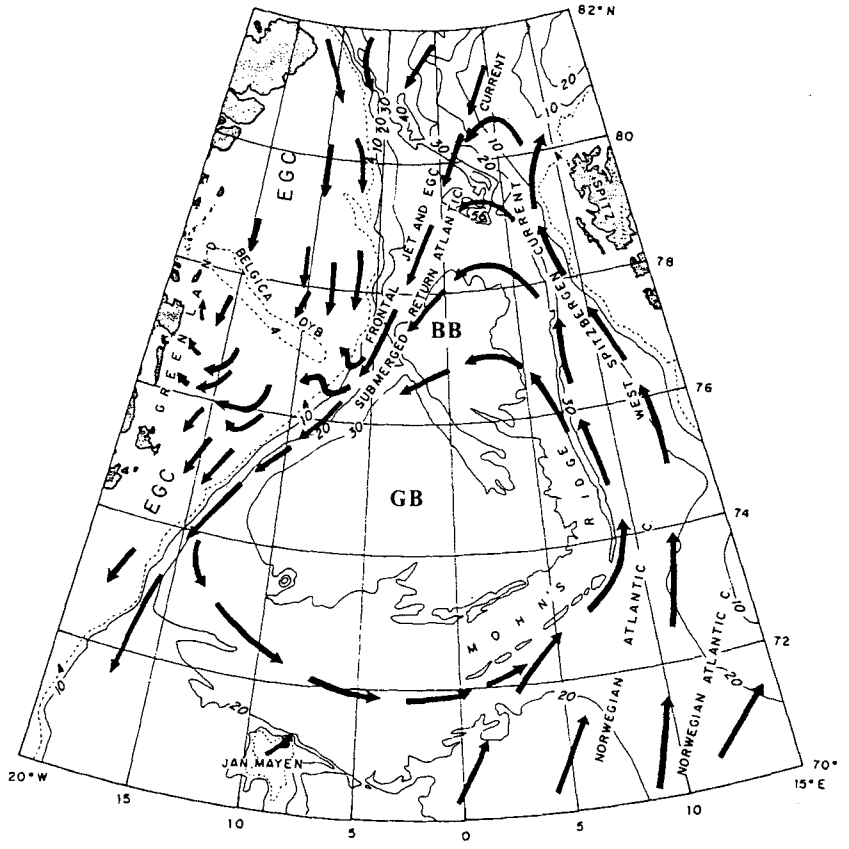

Fig. 2.1: Bathymetry and currents in the Greenland Sea. Depth labels are in hundreds of meters (BB= Boreas Basin, EGC= East Greenland Currrent, GB= Greenland Basin, modified from Paquette et al. 1985).

the arctic waters are not simply the product of mixing between the Polar and Atlantic Water (PW, AW), since they are much denser than any of the source waters and concludes that extensive modification must occur to account for the observed changes. Relatively high salinities and low Tritium concentrations in the Greenland Sea Gyre (GSG) indicate that PW contributes only little to the arctic waters (Swift and Aagard 1981). On the other hand, the steep horizontal gradients constituting the Arctic Front preclude extensive mixing of AW into the central gyre. This is taken as further evidence for AW having to undergo modification (cooling and sinking) before entering the arctic domain (Swift 1986). However, cross-frontal mixing of AW has been proposed by van Aken (1989) and van Aken et al. (1991), based on the occurrence of warm core eddies to the west of the front.

Within the arctic domain, the cyclonic circulation leads to a doming of the isopycnals and a reduced density stratification in the center of the gyre. A 20 to 40 m thick seasonally warmed layer with temperatures of about 4.5°C marks the surface of the GSG. This is Arctic Surface Water (ASW), with temperatures above 2°C and salinities ranging between 34.7 and 34.9 (Swift 1986). Below the seasonal pycnocline a second water mass is associated with the upper temperature minimum located between 75 and 150 m. This

upper Arctic Intermediate Water (UAIW) forms in fall and winter. Its salinity is determined by the depth of wintertime mixing. Lower Arctic Intermediate Water (LAIW) is associated with a marked temperature and salinity maximum located between 250 and ≥400 m. The temperatures are in the range of 0 to 3°C, and salinity is greater than 34.9 (Swift 1986). The property maxima are clear signs that this water mass is produced by the cooling and sinking of AW. Below these intermediate waters we find the Greenland Sea Deep Water (GSDW) which comprises about 85% of the volume of the Greenland Sea water masses (Carmack and Aagard 1973). It is the coldest and densest water in the Greenland Sea, with salinities typically between 34.88 and 34.90 and potential temperatures between -1.1 and -1.3°C (Swift 1986). It is believed to be formed by winter cooling and deep convection in the center of the GSG, resulting in a homogeneous water column from the surface to the bottom (Nansen 1906). However, such conditions have not (yet) been observed and other possible mechanisms of deep water formation have therefore been proposed (Metcalf 1955, Carmack and Aagard 1973, Clarke et al. 1990).

Water exchange

There have been several attempts to quantify the volume transport of the exchange flow between the Arctic Ocean and the North Atlantic, but the estimates are based on a variety of methods, many of which are not considered reliable in the oceanographic literature. A recent summary of estimates for the overflow into the North Atlantic across the sills in the Denmark Strait (620 m) and the Faroe Bank Channel (840 m) indicates a transport of 5.6 Sv[2] (Dickson et al. 1990). The main overflow occurs across the Denmark Strait (2.9 Sv) and is principally supplied by UAIW (Swift et al. 1980), whereas the overflow across the Faroe Bank Channel (1.7 Sv) consists primarily of Norwegian Sea Deep Water. Net outflow from the Arctic Ocean into the Greenland Sea (sill depth 2650 m) is estimated some 1.7 Sv (Rudels and Quadfasel 1991), of which a considerable portion (0.5 Sv) is Arctic Ocean Deep Water. Deep water can circulate freely within the Norwegian, Greenland and Eurasian basins, but it is confined by the shallow sills of the Greenland-Scotland ridge.

Ice cover

Permanent ice cover in the Greenland Sea is restricted to the polar waters west of the East Greenland Polar Front and consists mainly of multi-year ice originating from the Arctic Ocean (e.g. Wadhams 1986). Within the GSG, sea ice cover is seasonal and shows high interannual variability (Vinje 1977). A recurring feature, however, appears to be a tongue of pack extending into the area from the southwest and curling around the center of the GSG. This is the 'is odden' named by the Norwegian seal hunters, leaving an ice-free 'nordbukta' in its center. A plausible mechanism for the formation of this phenomenon has been recently proposed by Visbeck (1993).

Summary

The most important features of the physical setting relevant to the biological oceanography of the Greenland Sea can be summarized as follows:

[2] 1 Sv=10^6 $m^3 * s^{-1}$

- the surface connection to both, the Arctic Ocean and North Atlantic,
- the deep connection to the Arctic Ocean and Norwegian Sea,
- the vicinity of water masses of disparate origin and the hydrographic separation of polar, arctic and Atlantic domains,
- the slow and circular current regime within the arctic domain,
- the doming of isopycnals and vertical instability in the GSG,
- the recurrence of an ice-free 'nordbukta' in the center of the GSG.

3 Material and Methods

Sampling and sample processing

Large-scale regional and seasonal sampling was carried out during the 1988/89 field phase of the international Greenland Sea Project (GSP) and during spring of 1993 (Table 3.1).

Material for the regional study was collected during cruise Nr. 8 of RV „Meteor" in November 1988, occupying four stations on a zonal transect from Bear Island to the East Greenland Polar Front (Fig. 3.1, Table 3.1). All stations were ice-free at that time. The Arctic Front separated the Bear Island station 609 (12°57'E) in the West Spitsbergen Current (WSC) from the arctic stations in the gyre. Later sections will refer to the ensemble of stations of this cruise as *„regional"* or „zonal" transect across the *Greenland Sea* in *late fall*, to station 609 as „WSC" or simply „13°E".

Fig. 3.2 shows conspicuously different temperature and salinity profiles between 13°E and the arctic stations. In the arctic domain, cold low salinity Arctic Surface Water overlies a warm saline layer of Arctic Intermediate Water between 50 and 200 m (data are missing for the upper 50 m at station 616). The water column is nearly homogenous below (Greenland Sea Deep Water). The WSC (13°E) displays a complicated hydrographic structure with warm saline Atlantic water at the surface, and a series of cold and warm intrusions below, not giving way to a homogenous water column until about 1200 m.

For the seasonal study, the center of the Greenland Sea Gyre (GSG) was revisited on board RVs „Meteor", „Valdivia" and „Polarstern" in late fall, winter, early and late summer of 1988/89 and again in spring 1993 (Table 3.1). Later sections will address the ensemble of stations, excluding 609 and 616, as *„seasonal"* or „temporal" investigation in the *GSG*. For definition of seasons see Table 3.1. Stations 613, 653 and 8 are collectively referred to as „dark season" (November-February), stations 61, 91 and 177 as „light season" (April-

Table 3.1: Station data for deep Multinet hauls in the Greenland Sea, sampling the depth strata 3000 (or bottom)-2000-1500-1000-500-400-300-200-100-0 m (WSC= West Spitsbergen Current, GSG= Greenland Sea Gyre, EGPF= East Greenland Polar Front).

Station	RV	Cruise	Region	Position		Season	Date	Time range [h UTC]	Depth [m]
609	Meteor	8/1	WSC	74°45'N	12°57'E	late fall	06 Nov 88	22-02	2284
613	"	"	GSG	74°45'N	01°04'E	"	08 Nov 88	13-18	3777
616	"	"	EGPF	74°42'N	08°33'W	"	10 Nov 88	10-15	3352
653	"	8/2	GSG	74°06'N	03°02'W	"	27 Nov 88	18-22	3655
8	Valdivia	78/1	"	74°45'N	08°01'W	winter	07 Feb 89	22-05	3400
91	Polarstern	ARK VI/3	"	74°45'N	01°02'E	early summer	15 Jun 89	07-12	3770
177	Valdivia	86	"	74°45'N	01°04'E	late summer	18 Aug 89	14-18	3780
61	Polarstern	ARK IX/1b	"	75°00'N	02°38'W	spring	09 Apr 93	13-22	3688

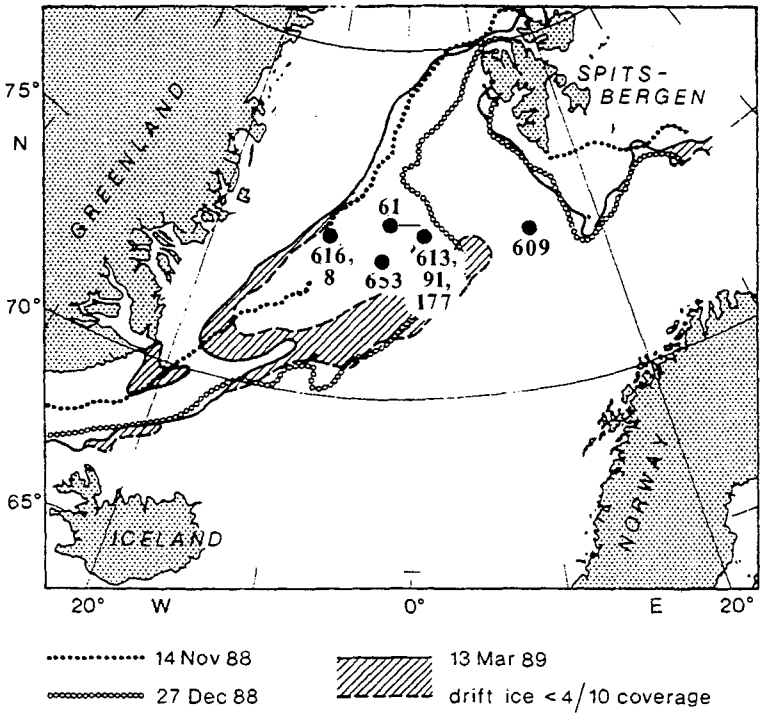

Fig. 3.1: Sampling locations and extent of ice-cover during the sampling period (modified from Fischer and Visbeck 1993).

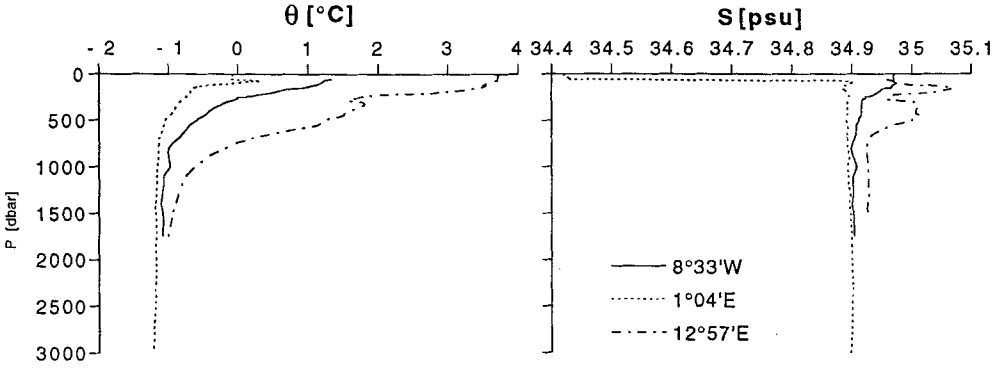

Fig. 3.2: Profiles of potential temperature (θ) and salinity (S) along the regional transect across the Greenland Sea in November 1988, at 8°33'W, 1°04'E (arctic domain) and 12°57'E (Atlantic domain), (uncalibrated data, courtesy of D. Quadfasel, IfM Hamburg).

August). Results are presented in chronological order, i.e. beginning with late fall of 1988 (station 613) and ending with late summer of 1989 (station 177). The only exception is spring (station 61) which is from a different year (1993). Temperature and salinity profiles for the 1988/89 period in the GSG are given in Fig. 3.3. They show pronounced modifications of ASW and AIW in course of the year which may extend down to about 1800 m.

Sampling equipment and design was identical throughout the entire investigation. Zooplankton was sampled from 3000 m (or sea bed, 13°E) to the surface, deploying a Kiel Multinet equipped with five nets (150 µm mesh) in two successive vertical hauls from 3000 m (or bottom) and 500 m to the surface. Sampling intervals were 3000 (or bottom)-2000-1500-1000-500-0 m for the deep hauls, and 500-400-300-200-100-0 m for the shallow casts. Clogging never was a problem and filtered volume was calculated from wire length and Multinet mouth area (0.25 m^2), assuming 100% filtering efficiency at 0.3-0.5 $m*s^{-1}$ hauling velocity. Samples were preserved in 4% borax-buffered formaldehyde.

Part of the material was shared with other investigators, who kindly made available their data and samples to this study (Table 3.2).

For species identification, specimens were dissected under a stereo microscope and determined under high magnification (up to 400*) in the microscope. Reference was made to the extensive taxonomic literature cited in Mumm (1991, pp. 22-25), furthermore to Sars (1903), Heptner (1971), Park (1978), Brodskii et al. (1983), Nishida (1985), Frost (1989), and Koszteyn and Kwasniewski (1991) for copepods; to Weslawski (1991) for amphipods, and to Herman and Andersen (1989) for pteropods.

Samples were sorted in a Bogorov plate under a stereo microscope with dark and bright field illumination. As a rule, the entire sample was enumerated for the larger plankton (>1 mm), and only occasionally the sample was split with a Folsom splitter (1:2) for quantification of very abundant species or stages. Routine identification was usually to the

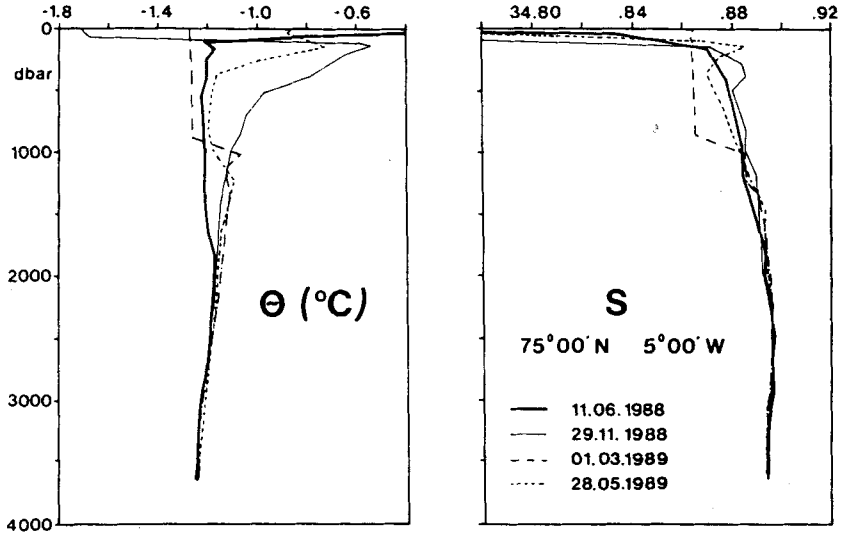

Fig. 3.3: Profiles of potential temperature (θ) and salinity (S) in the central Greenland Basin in early summer 1988, late fall 1988, winter 1989 and early summer 1989 (from GSP Group 1990).

Table 3.2: Stations and taxa and for which abundance data were provided, courtesy of H.-J. Hirche, T. Scherzinger and R. Weigmann-Haass.

St.	*Calanus* spp.	*Metridia longa*	Ostracoda	Hyperiidae	Euphausiacea	Chaetognatha
609	*Hirche 1991	†Hirche 1991	Haass unpubl.	Haass unpubl.	Haass unpubl.	**Hirche unpubl.
613	"	Scherzinger 1994	"	"	"	"
616	"	†Hirche 1991	"	"	"	"
653	"	Scherzinger 1994	"	"	"	"
8	*‡Hirche unpubl.	†Hirche unpubl.				
91	"	"				**Hirche unpubl.
177	"	"				"

* and † denote missing values for copepodite stages CI-CII and CI-CIII, respectively; ‡= no separation between *Calanus finmarchicus* and *C. glacialis* for all stages; **= including length data

species level and most of the larger calanoid copepods were further separated into copepodite stages. For the small plankton (<1 mm), an aliquot (1:2, 1:4, 1:10, exceptionally 1:100) of the sample was counted after fractionation with a Folsom or Wiborg splitter. Only metazoans were counted. Cyclopoid copepods were sorted to the genus. Taxonomic identification of the smallest calanoids (*Microcalanus pygmaeus, M. pusillus, Spinocalanus* spp.) and of calanoid nauplii was not attempted on a routine basis. The latter were recorded as „small calanoids" and „nauplii", respectively. Subsequent length measurements via digital image analysis allowed to delimit *a posteriori* taxonomic entities from the occurrence of multiple modes in the length-frequency distributions. This was verified microscopically for *Oithona* and *Oncaea* at the species level and for *Pseudocalanus* and *Boroecia* at the stage level, as will be shown later.

Image analysis

Computer analysis of digitized video images was performed with an unpublished image analysis software ('BILD') developed by W. Hukriede (IfM, Kiel) on a NeXT workstation. Specimens were placed in calibrated measuring vials and videotaped with a S-VHS camera equipped with a macro lens. The processing involved digitizing, scaling and measuring of the image on the computer screen by means of a 'mouse'. The procedure is semi-automatic and fast, allowing for several hundred measurements per hour. Damaged specimens as well as those which were off-axis or out of focus were excluded. Repeated measurements of 25 individuals of *Oncaea* (0.6 mm total length) yielded a precision of 3.4% of the mean. This is probably a 'worst case scenario', since usually tens to hundreds of animals were measured per sample. Furthermore, precision increases with organism size. Prosome lengths (i.e. from the tip of the rostrum to the median articulation between prosome and urosome) were measured for calanoid copepods and total lengths (i.e. largest extension excluding projections) for all other taxa. Line measurements were performed in most cases, but polygones or curves were applied on bent animals [*Oncaea*, amphipods and (often) chaetognaths]. Data were stored in spreadsheet files for subsequent length-frequency analysis.

Length-frequency histograms were plotted to visualize vertical and seasonal shifts in the length distribution of the assemblage. Lower mode distributions were the rule, and modes were traced by eye to follow vertical or seasonal increments in length.

Biomass calculation

Plankton material for direct biomass determinations was not available for this investigation. Biomass was therefore calculated from published and unpublished taxon-specific weight-length relationships, individual dry weights (DW_i), stage- and length composition and numbers of individuals in the samples (APPENDIX 1). The compiled DW_i are from fresh or frozen GSG material, ideally, and from formaline samples outside the area, at the worst. They are given as somewhat bold averages but standard deviations are provided as a measure of variance within the source data.

Statistical analysis

The regional, seasonal and vertical centers of distribution were calculated according to Mumm (1991). Species were ranked depending on their centers of distribution in order to display the distribution patterns in the tabular fashion introduced by Mumm (1991, 'Mumm-plot', Figs. 4.16-18).

To display the seasonal changes in the vertical distribution of abundance and biomass, the z_{50} depths were calculated. These are the depths above which 50% of the population is distributed (cf. Fig 4.14), assuming a homogeneous distribution within each sampling interval. For the biomass-dominating taxa, the z_{05}, z_{25}, z_{75} and z_{95} depths were calculated accordingly. The vertical biomass distribution of these taxa is depicted in box plots, each box encompassing 50% of the population, in terms of biomass (cf. Figs. 4.37, 4.55 and 4.59).

The similarities between the samples in terms of faunistic composition were examined by the ANOSIM permutation test (Clarke and Warwick 1994) as well as classification and ordination techniques as proposed by Field et al. (1982). These non-parametric multivariate methods were performed on a data matrix of 39 rows (taxa) and 54 columns (samples) comprising the recurring taxa of all samples from the temporal study. All three analyses were based on Bray-Curtis similarities (Bray and Curtis 1957) between sample pairs computed on fourth-root transformed abundances, following the recommendations of Clarke and Green (1988) (transformations) and Faith et al. (1987) (similarity coefficients). The matrix of similarities was used to test for vertical and seasonal differences between the samples. Subsequently, the samples were classified by hierarchical agglomerative clustering with group-average linking (e.g. Clifford and Stephenson 1975) and mapped according to their faunistic similarities in an ordination by non-metric multidimensional scaling (MDS, e.g. Kruskal and Wish 1978). Classification and ordination was repeated after transposing the abundance matrix and computing a similarity matrix between every pair of species, in order to examine the inter-relationships between the species.

While clustering and MDS are explorative statistical methods, Clarke and Warwick (1994) recently introduced a formal test to establish statistical assemblage differences between sites, times, etc. This ANOSIM test (in analogy to ANOVA) covers the case of a two-way crossed layout of samples *without* replication, in which „treatments" (here: depths) are replicated only once within each „block" (here: seasons). The crossed design

arises when e.g. the samples are taken from a set of depth intervals at a number of seasons, the term „crossed" implying that for each season there are observations from the same set of depth intervals. The test yields significance levels for the overall presence of treatment effects (depth), based on a measure of concordance within each block (season). The factors are reversed to obtain a test for block effects. For the purpose of this study the following null hypotheses were tested:

H_{01}: there are no seasonal effects in community patterns among the samples (but allowing for the possibility of depth differences)

H_{02}: there are no depth differences (but allowing for possible seasonal effects).

The average Spearman's correlation ρ_{av} is calculated as a measure of concordance and its significance is examined by a permutation test: if the observed ρ_{av} is greater than e.g. in all 999 of 1000 permutated simulations, the null hypothesis can be rejected at a significance level of 0.1% ($p<0.001$). 5000 permutations were carried out in the present study.

All computations were performed with the PRIMER programs (Plymouth Routines in Multivariate Ecological Research) developed at Plymouth Marine Laboratory.

Standard measures are given for species numbers (S), diversity (H') and evenness (J) of samples (Shannon and Weaver 1963, Pielou 1969).

4 Results

The first part of this section will give an overview of the qualitative and quantitative results from the regional and seasonal investigation, including species composition, total abundance and biomass, before leading over to species distribution and multivariate analyses of community patterns. Finally, dominant species as well as species representing a particular distribution type will be highlighted.

Within each chapter, the integrated values (on a square meter basis) of the regional and seasonal study are presented first, followed by the vertical distributions (on a cubic meter basis) encountered during the regional and seasonal investigation.

4.1 General overview

Species numbers and diversity

A total of 67 taxa belonging to seven phyla are reported for this study (Table 4.1). 61 species were identified, nine of which are recorded at the generic level. Including sexes and developmental stages, a total of 145 categories were enumerated.

Most species are listed for calanoid copepods (28), followed by cyclopoids (6), hydromedusans and siphonophores (each 5).

The regional and seasonal variations in species numbers (S) and diversity (H') are given in Figs. 4.1 and 4.2.

Along the zonal transect across the Greenland Sea in late fall, the highest numbers of species are found in the center of the gyre (1°E and 3°W, S=48-49), while at the East Greenland Polar Front (8°30'W) and in the West Spitsbergen Current (WSC, 13°E) only 41 and 40 are recorded, respectively (Fig. 4.1). The diversity index (H') appears to be rather unrelated to the number of species present and is higher on the two eastern stations. At 13°E the diversity maximum coincides with the species minimum.

Species numbers in the Greenland Sea Gyre (GSG) vary seasonally between 44 and 52 (February, April; Fig. 4.2). Diversity (H')

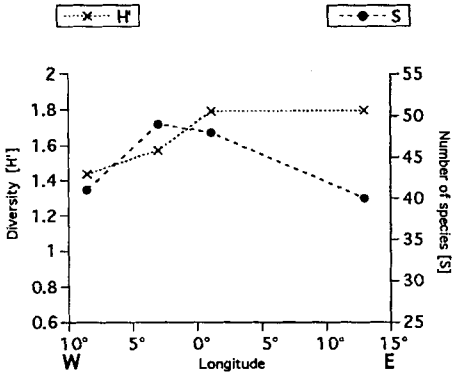

Fig. 4.1: Regional distribution of diversity [H'] and species number [S] across the Greenland Sea (75°N) in November 1988 (cf. Table 3.1 for station data).

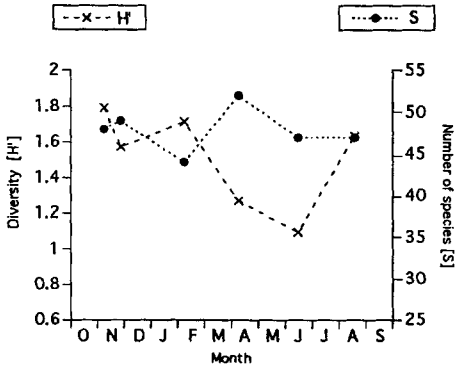

Fig. 4.2: Seasonal distribution of diversity [H'] and species number [S] in the Greenland Sea Gyre.

again follows a different pattern, with a pronounced minimum in spring and early summer. The correlation of Shannon-Wiener diversity (H') versus species numbers for all samples yields a 'shotgun plot' (Fig. 4.3), corroborating the earlier observation that species numbers contribute only little to diversity. Figure 4.4 shows that diversity is rather determined by the evenness (J'), low values representing an uneven distribution of individuals among species, i.e. dominance of a few species.

The vertical distribution of S and H' from 0-3000 m, pooled for all seasons, shows a steady increase of both parameters from the surface to 1000-1500 m, followed by a

Table 4.1a: Species list of copepods in the Greenland Sea (cf. Figs. 4.16-4.18 for regional, seasonal and vertical distributions).

Species	Family	Copepodite stages
Calanoida		
Calanus finmarchicus (Gunnerus)	Calanidae	CIII-CVI
Calanus glacialis Jashnov	"	"
Calanus hyperboreus Krøyer	"	"
Microcalanus pygmaeus (Sars)	Pseudocalanidae	-
Microcalanus pusillus Sars	"	-
Pseudocalanus minutus (Krøyer)	"	-
Spinocalanus horridus Wolfenden	Spinocalanidae	-
Spinocalanus spp.	"	-
Aetideopsis multiserrata Wolfenden	Aetideidae	CI-CVI
Aetideopsis rostrata Sars	"	"
Chiridiella abyssalis Brodskii	"	CVI
Chiridius obtusifrons Sars	"	CI-CVI
Gaidius brevispinus (Sars)	"	"
Gaidius tenuispinus (Sars)	"	"
Undeuchaeta spectabilis Sars	"	CVI
Euchaeta barbata Brady	Euchaetidae	CVI
Euchaeta farrani With	"	"
Euchaeta glacialis Hansen	"	"
Euchaeta norvegica Boeck	"	"
Euchaeta cf. *polaris* (Brodskii)	"	"
Euchaeta spp.	"	CI-CV
Scaphocalanus brevicornis Sars	Scolecithricidae	≤CV, CVI
Scaphocalanus magnus (Scott)	"	"
Scolecithricella minor Brady	"	-
Metridia longa (Lubbock)	Metridiidae	CI-CVI
Heterorhabdus compactus Sars	Heterorhabdidae	≤CV, CVI
Heterorhabdus norvegicus (Boeck)	"	CI-CVI
Lucicutia polaris Brodskii	Lucicutiidae	CVI
Augaptilus glacialis Sars	Augaptilidae	CVI
Haloptilus acutifrons (Giesbrecht)	"	CVI
Cyclopoida		
Mormonilla sp.	Mormonillidae	-
Oithona atlantica Farran	Oithonidae	-
Oithona similis Claus	"	-
Oncaea borealis (Sars)	Oncaeidae	-
Oncaea curta (Sars)	"	-
Oncaea cf. *similis* (Sars)	"	-
Harpacticoidea		
Microsetella norvegica Boeck	Ectinosomidae	-

Table 4.1b: Species list of other zooplankton taxa (cf. Figs. 4.16-4.18 for regional, seasonal and vertical distributions).

Species	Family	
Amphipoda		
Themisto abyssorum (Boeck)	Hyperiidae	
Themisto libellula (Lichtenstein)	"	
Ostracoda		
Boroecia borealis (Sars)	Halocyprídae	
Discoconchoecia elegans (Sars)	"	
Isopoda		
isopod larvae	Bopyridae	
Euphausiacea		
Thysanoessa inermis Krøyer)	Euphausiidae	
Thysanoessa longicaudata (Krøyer)	"	
Meganyctiphanes norvegica (Sars)	"	
Decapoda		
Hymenodora glacialis (Buchholz)	Oplophoridae	
Polychaeta		
indet.		
Pteropoda		
Clione limacina (Phillips)	Clionidae	
Limacina helicina (Phillips)	Limacinidae	
Limacina retroversa (Fleming)	"	
Appendicularia		
Oikopleura vanhoeffeni Lohmann	Oikopleuridae	
Chaetognatha		
Eukrohnia bathypelagica Alvariño		
Eukrohnia hamata (Möbius)		
Heterokrohnia mirabilis Ritter-Záhony		
Sagitta maxima (Conant)		
Siphonophora		
Crystallophyes amygdalina Moser	Chuniphyidae	ant./post. nect.
Dimophyes arctica (Chun)	Diphyidae	ant./post. nect., eudoxia
Lensia reticulata Totton	"	eudoxia
Muggiaea bargmannae Totton	"	nect, eudoxia
Marrus orthocanna (Kramp)	Agalmidae	-
Hydromedusae		
Aegina citrea Eschscholtz	Aeginidae	
Aglantha digitale (Müller)	Rhopalonematidae	
Crossota norvegica Vanhoeffen	"	
Botrynema brucei Browne	Halicreatidae	
Botrynema ellinorae Hartlaub	"	
Botrynema sp.	"	
Scyphomedusae		
Atolla wyvillei Haeckel	Atollidae	
Ctenophora		
indet.		

ant.= anterior, post.= posterior, nect.= nectophore

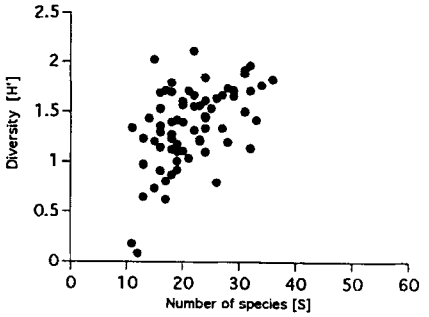

Fig. 4.3: Diversity [H'] versus species number [S] for all samples.

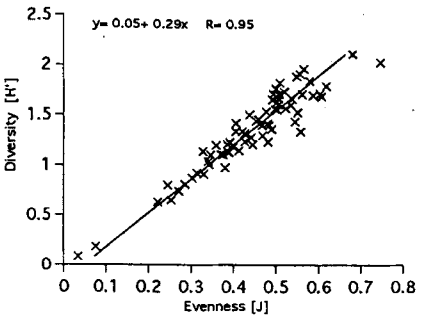

Fig. 4.4: Diversity [H'] versus evenness [J] for all samples.

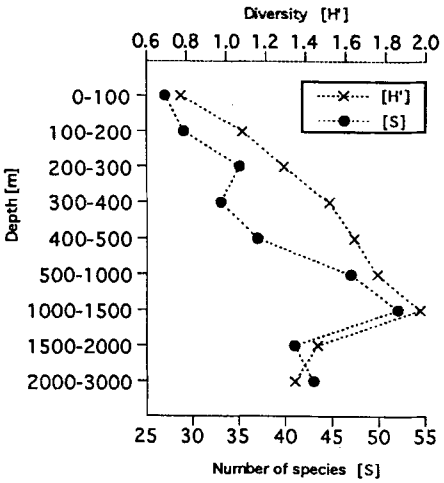

Fig. 4.5: Diversity [H'] and species number [S] versus depth. Species numbers are pooled for each depth stratum over all seasons. Note the scale break at 500 and 2000 m.

marked drop below (Fig. 4.5). Correlation plots show that both, species numbers and evenness contribute to diversity (Figs. 4.6 and 4.7). I.e., few species predominate at the surface, while in the upper bathypelagial high species numbers coincide with an even distribution of individuals among species. It will be a matter of discussion whether the observed vertical pattern, e.g. the intermediate maximum, is spurious (sampling bias) or 'real' (seasonal vertical migrations).

Total zooplankton

Regional and seasonal variations of abundance and biomass, integrated over a

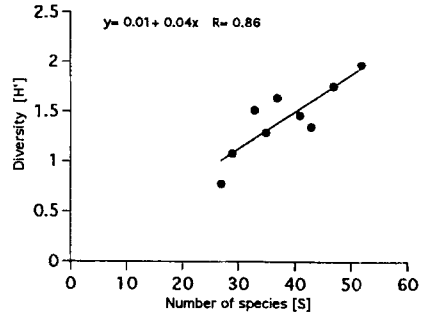

Fig. 4.6: Diversity [H'] versus species number [S] pooled for each depth stratum over all seasons.

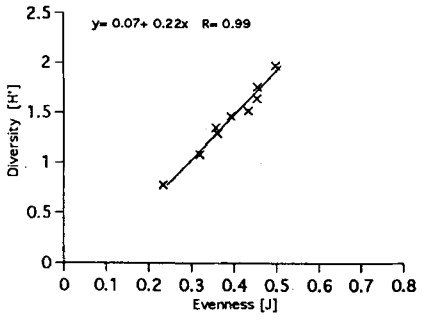

Fig. 4.7: Diversity [H'] versus evenness [J] pooled for each depth stratum over all seasons.

3000 m water column, are shown in Figs. 4.8 and 4.9.

The zonal transect along 74°45'N in late fall shows only moderate changes in both parameters (Fig. 4.8). No pattern emerges for the abundances, except for a drop in the WSC (13°E). The numbers here ($0.7*10^5$ $n*m^{-2}$) are markedly lower than the values in the gyre [$(3\pm1)*10^5$ $n*m^{-2}$]. Biomass, by contrast, is remarkably constant along the section, the standard deviation is only 7% of the mean (13±1 g $DW*m^{-2}$). The apparent disparity between biomass and abundance is due to differences in species and stage/size distributions, as will be shown later.

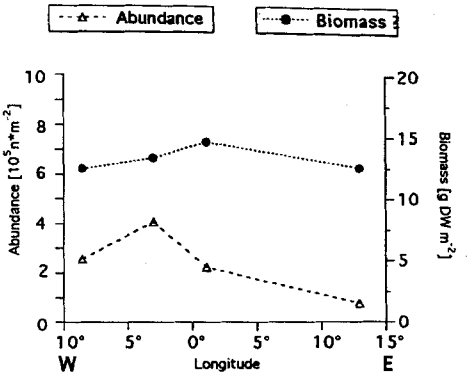

Fig. 4.8: Regional distribution of abundance and biomass in the Greenland Sea (75°N) in November 1988.

Overall variability is greater in the GSG on a seasonal scale (Fig. 4.9). A sharp abundance peak of $7.4*10^5$ $n*m^{-2}$ in June towers above a more or less constant level of (3.0 ± 0.8) $*10^5$ $n*m^{-2}$ during the rest of the year. Biomass follows a much smoother curve, describing a sinusoid around 14 $g*m^{-2}$ with a small amplitude of 3 $g*m^{-2}$. The seasonal biomass minimum coincides with the abundance minimum in February. The biomass maximum, however, is out of phase with the abundance peak and occurs later in summer, at a time when abundance values have again dropped to winter levels. It will be shown in the following that different organisms account for the observed abundance and biomass changes in the GSG.

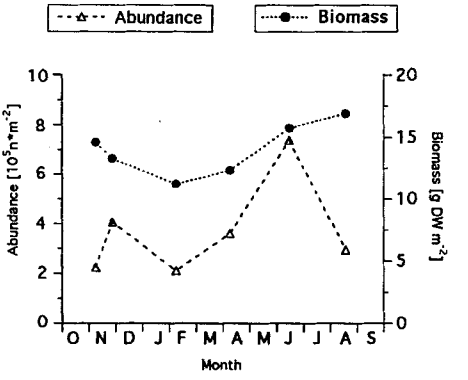

Fig. 4.9: Seasonal distribution of abundance and biomass in the Greenland Sea Gyre.

Mean vertical distributions of abundance and biomass

Vertical distributions of regionally and seasonally averaged zooplankton abundance and biomass are shown in Figs. 4.10 and 4.11.

The regional mean shows a general but moderate decrease of abundance with depth of one order of magnitude from the surface to the deep sea (>1000 m, Fig. 4.10a). However, this decrease is not monotonous, as evidenced by a subsurface peak in the lower epipelagial[3] (200-300 m). A subsurface feature is also apparent in the vertical distribution of biomass, albeit deeper in the water column (400-500 m, Fig. 4.10b). Biomass remains high down to the upper reaches of the bathypelagial (1500 m), at about half the concentration of the surface layer.

Averaged over the whole year, highest densities of both, individuals and dry weights are found at the surface (Fig. 4.11). Variability in this layer is also highest, and the standard

[3] According to the terminology proposed by Omori and Ikeda (1984), the epipelagic zone extends from the surface down to 300 m, the mesopelagic zone from 300 to 1000 m and the bathypelagic from 1000 to 3000 m. The 150 m and 700 m marks separate the upper and the lower epi- and mesopelagial, respectively.

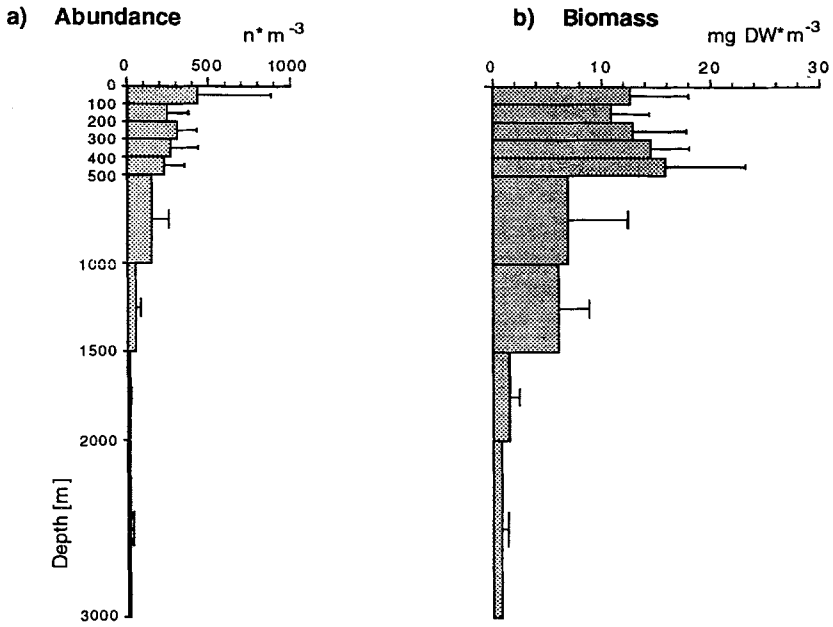

Fig. 4.10: Vertical distribution of abundance (a) and biomass (b), regional average across the Greenland Sea (75°N) in November 1988. Error bars denote standard deviations.

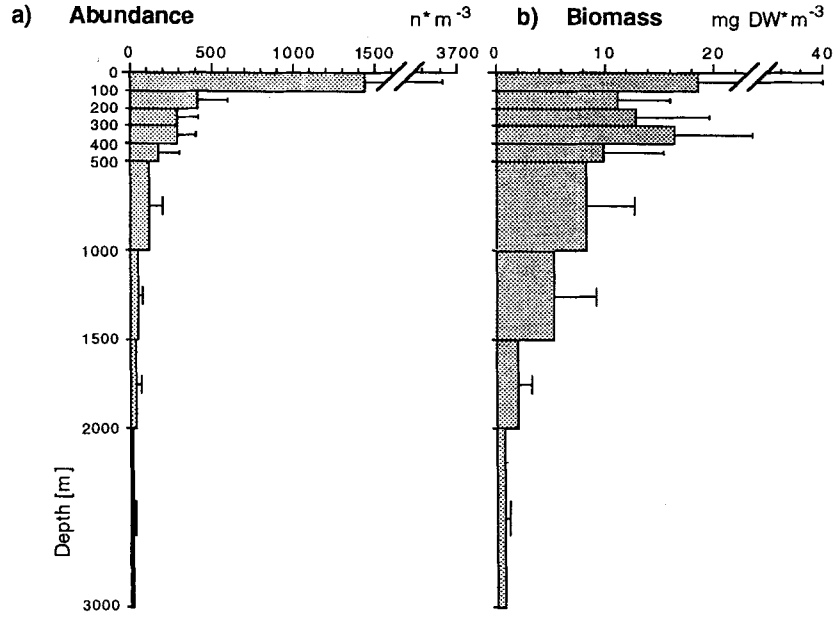

Fig. 4.11: Vertical distribution of abundance (a) and biomass (b), annual mean across the Greenland Sea Gyre. Error bars denote standard deviations. Note the scale breaks for the top 100 m.

deviation of the abundance values exceeds 1.5 times the mean. Abundances plummet along the vertical over two orders of magnitude between the surface and the deep sea.

The decline is less dramatic in terms of biomass (about one order of magnitude, Fig. 4.11b) but appears to be superimposed by a subsurface peak located in the upper mesopelagial (300-400 m). A similar feature has already been described for late fall (see above).

Vertical distributions of abundance and biomass

The vertical distribution of abundance and biomass along the zonal section through the Greenland Sea in late fall is shown in Fig. 4.12. At the westernmost station (08°33'W) abundance is highest in the surface layer and decreases exponentially with depth (Fig. 4.12a). No such pattern is evident for the other stations, where the maxima are located deeper in the water column, between 100 and 500 m.

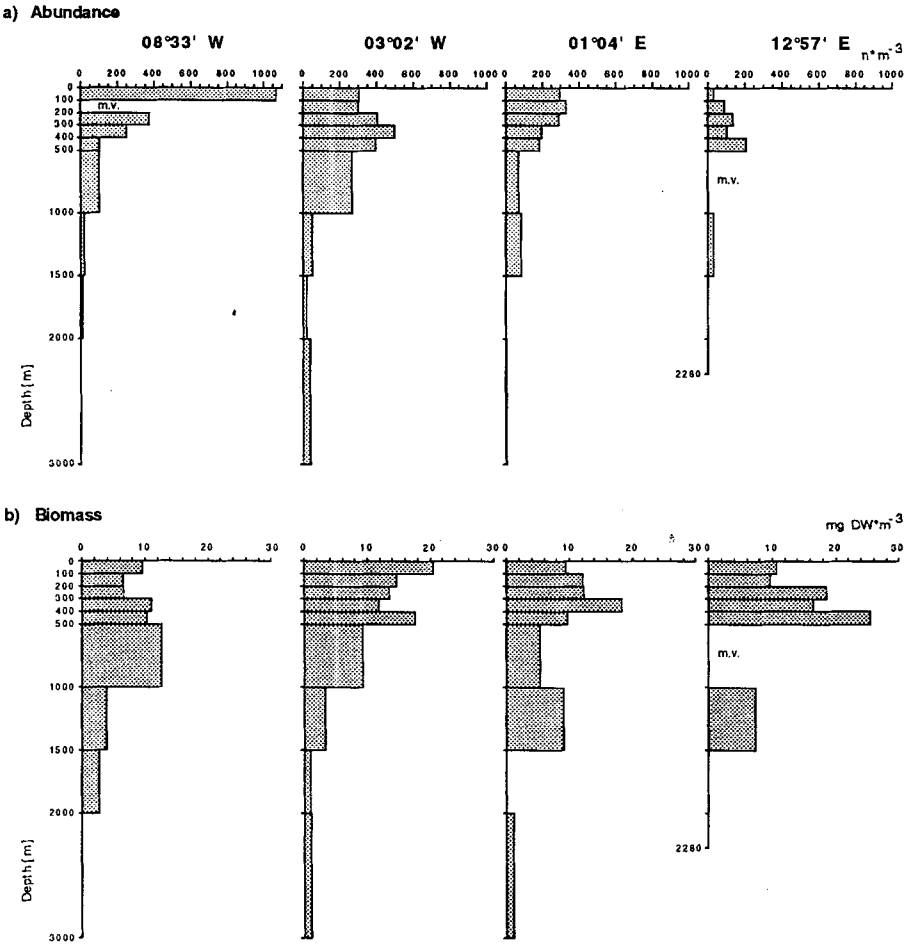

Fig. 4.12: Vertical distributions of abundance (a) and biomass (b) across the Greenland Sea (75°N) in November 1988 (m.v.= missing values for all taxa or those taxa not listed in Table 3.2).

In terms of biomass there is no conspicuous trend (Fig. 4.12b). The highest concentrations are usually found in the upper 1000 m, but no clear vertical pattern is discernible.

The temporal sequence of events underlying the average yearly pattern (presented in the foregoing chapter) reveals considerable changes in the vertical distribution of abundance and biomass in course of the year (Fig. 4.13). The dark season is characterized by only weak vertical gradients of abundance and biomass, leading to a more or less homogeneous distribution of these parameters in early February. The light season, by contrast, shows a surface-biassed vertical structure culminating in a highly aggregated distribution with maximum concentrations in the early summer surface layer (15 June). However, the abundance maximum precedes the biomass maximum and persists longer, whereas the biomass peak seems to be a rather ephemeral surface feature which desintegrates rather early, by the end of the summer season (18 August).

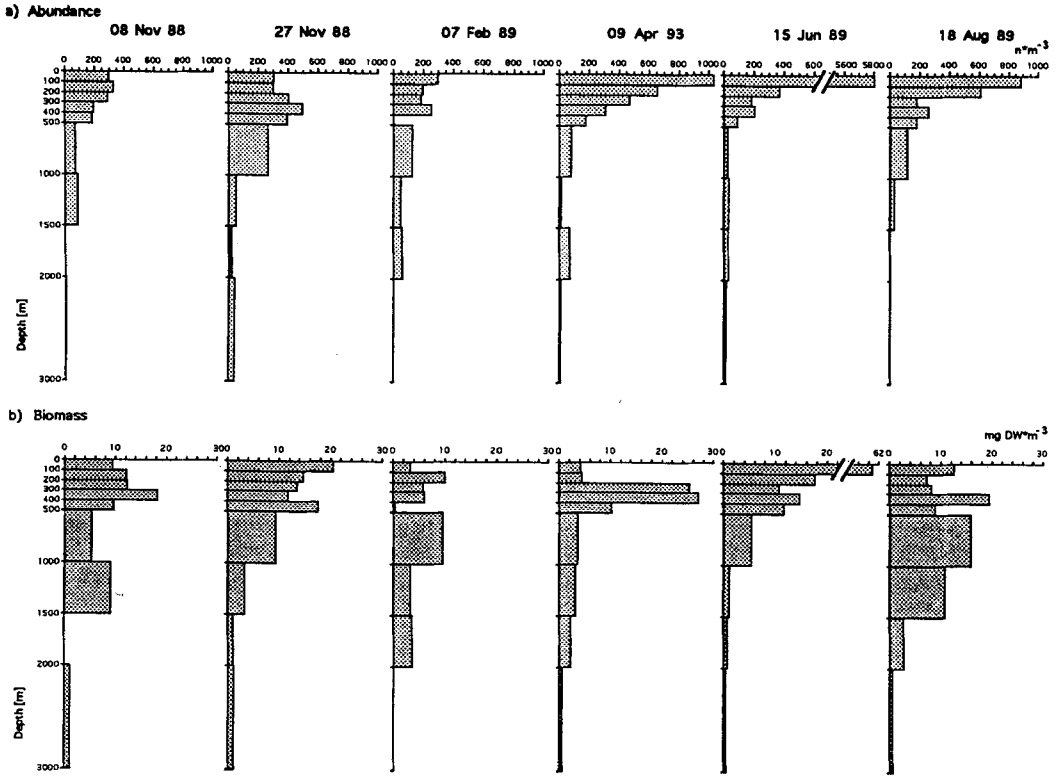

Fig. 4.13: Vertical distributions of abundance (a) and biomass (b) in the Greenland Sea Gyre in the course of the year. Note the scale breaks for 15 June 89.

Figure 4.14 shows the seasonal translocation of the depths of median zooplankton occurrence, in terms of abundance and biomass, where 50% of all specimens or biomass are above, and 50% below that depth. Both curves agree in phase and amplitude with seasonal extremes in February and June and vertical ranges of about 600 m. They are, however, separated in space, as evidenced by the shallower distribution of abundance relative to biomass.

This is a further indication of marked differences in the species and size contributions to zooplankton abundance and biomass in the Greenland Sea.

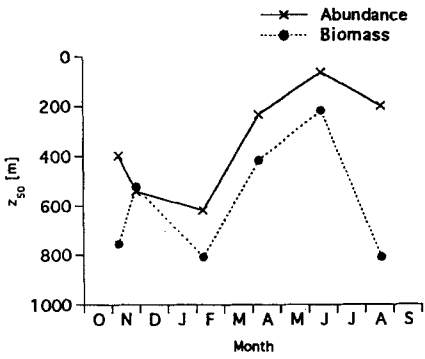

Fig. 4.14: Seasonal translocation of z_{50} depths of total zooplankton abundance and biomass in the Greenland Sea Gyre. These are the depths above which 50% of the population is distributed.

Relative composition of zooplankton abundance and biomass

Table 4.2 lists the „top ten" contributors to abundance and biomass, respectively, in rank order of importance on a regional and and annual basis. Obviously, only few but very different species account for the observed abundance and biomass changes. *Oithona* alone [almost exclusively *O. similis* (Cyclopoida, Copepoda)] accounts for more than half of total numbers, whereas *Calanus hyperboreus* (Calanoida, Copepoda) dominates the biomass, making up about one third of the yearly total biomass. Conversely, *C. hyperboreus* ranks only fifth in abundance (3%) and *O. similis* sixth in biomass (4%). This shows, that total abundance and biomass are largely independent measures of zooplankton stocks in the Greenland Sea. The numerical dominance of copepods is overwhelming. Abundance ranks one to seven on both, a regional and annual basis, are occupied by copepods, accounting for 97% of total numbers. The most numerous taxa are also the smallest, as illustrated by the inverse relationship between the yearly mean abundances and mean individual dry weights of the species set in question (Fig. 4.15).

In terms of biomass, the relative composition is somewhat less dominated by copepods, for the chaetognath *Eukrohnia* (chiefly *E. hamata*) ranks second and the ostracod *Boroecia borealis* third, amounting to roughly one fourth of the share (22% and 6%).

Table 4.3 summarizes the yearly averaged relative importance of the major taxonomic groups in the GSG. Two thirds of total numbers are cyclopoid copepods, slightly less than a third are calanoid copepods, and the remainder (<2%) are other taxa. Calanoids and cyclopoids make up about two thirds of the biomass (58%

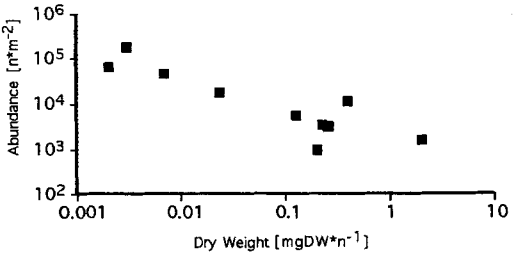

Fig. 4.15: Taxon-specific abundance versus mean individual dry weight, for the 'top ten' contributors to abundance in the Greenland Sea (cf. Table 4.2).

and 5%), other crustaceans add another 18%, chaetognaths 14%, and other taxa the remaining <6%.

Temporal variability in relative composition is below 10% of the mean for the main abundance and biomass constituents. Regional variability is higher (>20% and >10%,

Table 4. 2: 'Top ten' species in terms of total abundance and biomass in the Greenland Sea [incidental large macroplankton (*Atolla*, *Hymenodora*) excluded from biomass].

Abundance

Taxon	regional mean (%)	Taxon	annual mean (%)
Oithona spp.	44.3	*Oithona* spp.	53.3
Oncaea spp.	19.4	*Oncaea* spp.	19.2
small calanoids (*Microcalanus*)	15.7	small calanoids (*Microcalanus*)	13.6
Pseudocalanus minutus	5.9	*Pseudocalanus minutus*	5.0
Calanus finmarchicus	4.8	*Calanus hyperboreus*	3.4
Calanus hyperboreus	4.6	*Metridia longa*	1.6
Metridia longa	1.7	*Calanus finmarchicus*	1.0
Boroecia borealis	0.9	*Boroecia borealis*	0.9
Eukrohnia spp.	0.7	*Eukrohnia* spp.	0.5
Oikopleura vanhoeffeni	0.3	*Oikopleura vanhoeffeni*	0.3
other	1.7	other	1.2

Biomass

Taxon	regional mean (%)		annual mean (%)
Calanus hyperboreus	25.7	*Calanus hyperboreus*	31.8
Eukrohnia spp.	24.5	*Eukrohnia* spp.	21.9
Calanus finmarchicus	17.4	*Boroecia borealis*	5.5
Boroecia borealis	5.5	*Calanus finmarchicus*	5.3
Thysanoessa longicaudata	3.5	*Metridia longa*	4.7
Metridia longa	2.7	*Oithona* spp.	3.7
Pseudocalanus minutus	2.4	*Pseudocalanus minutus*	2.8
Oithona spp.	2.2	small calanoids (*Microcalanus*)	2.2
small calanoids (*Microcalanus*)	1.8	*Thysanoessa inermis*	1.6
Euchaeta spp.	1.6	*Euchaeta* spp.	1.6
other	12.7	other	18.9

respectively), due to a shift in numerical dominance from cyclopoid to calanoid copepods in the WSC, leaving them 59% and 75% of abundance and biomass, respectively (not shown in Table 4.3).

Table 4.3: Relative importance of major taxonomic groups in terms of total abundance and biomass in the Greenland Sea (means ± standard deviations).

Abundance

Taxon	regional mean %	Taxon	annual mean %
Cyclopoida	61.8±13.4	Cyclopoida	67.9±6.6
Calanoida	35.8±11.7	Calanoida	30.5±6.3
Ostracoda	0.9±0.4	Ostracoda	0.8±0.3
Chaetognatha	0.6±0.4	Chaetognatha	0.3±0.2
Pteropoda	0.3±0.8	Appendicularia	0.3±0.3
Appendicularia	0.3±0.2	Amphipoda	0.1±<0.1
Amphipoda	0.1±<0.1	Pteropoda	0.1±0.2
Euphausiacea	0.1±0.1	other	<0.1
other	<0.1		

Biomass

Taxon	regional mean %		annual mean %
Calanoida	61.7±8.6	Calanoida	58.2±5.0
Chaetognatha	16.0±5.9	Chaetognatha	13.6±4.8
Ostracoda	6.3±2.2	Ostracoda	6.1±1.7
Euphausiacea	5.5±2.2	Cyclopoida	5.1±2.6
Cyclopoida	3.1±1.7	Decapoda	4.6±3.7
Amphipoda	2.4±0.5	Euphausiacea	3.8±2.2
Pteropoda	2.0±1.8	Amphipoda	3.0±0.6
Hydromedusae	1.4±0.9	Hydromedusae	3.0±1.1
Appendicularia	1.1±0.9	Appendicularia	1.4±3.0
Siphonophora	0.5±0.2	Pteropoda	0.6±1.1
other	<0.1	Siphonophora	0.5±0.2
		Polychaeta	0.1±<0.1
		Isopoda	<0.1

Horizontal and vertical distribution patterns of abundance

Figure 4.16 displays the regional distribution pattern of copepods and other taxa in late fall, in the tabular fashion introduced by Mumm (1991, 'Mumm-plot', cf. Material and methods, p. 11). Species are ranked according to their zonal centers of distribution: taxa with a westerly distribution are listed in the upper, those with an easterly distribution in the lower part of the panel. The former case is represented by *Oithona*, which thrives west of the prime meridian, the latter by *Calanus finmarchicus* (Fig. 4.16a), the ostracod *Discoconchoecia elegans* and the pteropod *Limacina retroversa* (Fig. 4.16b), which are more

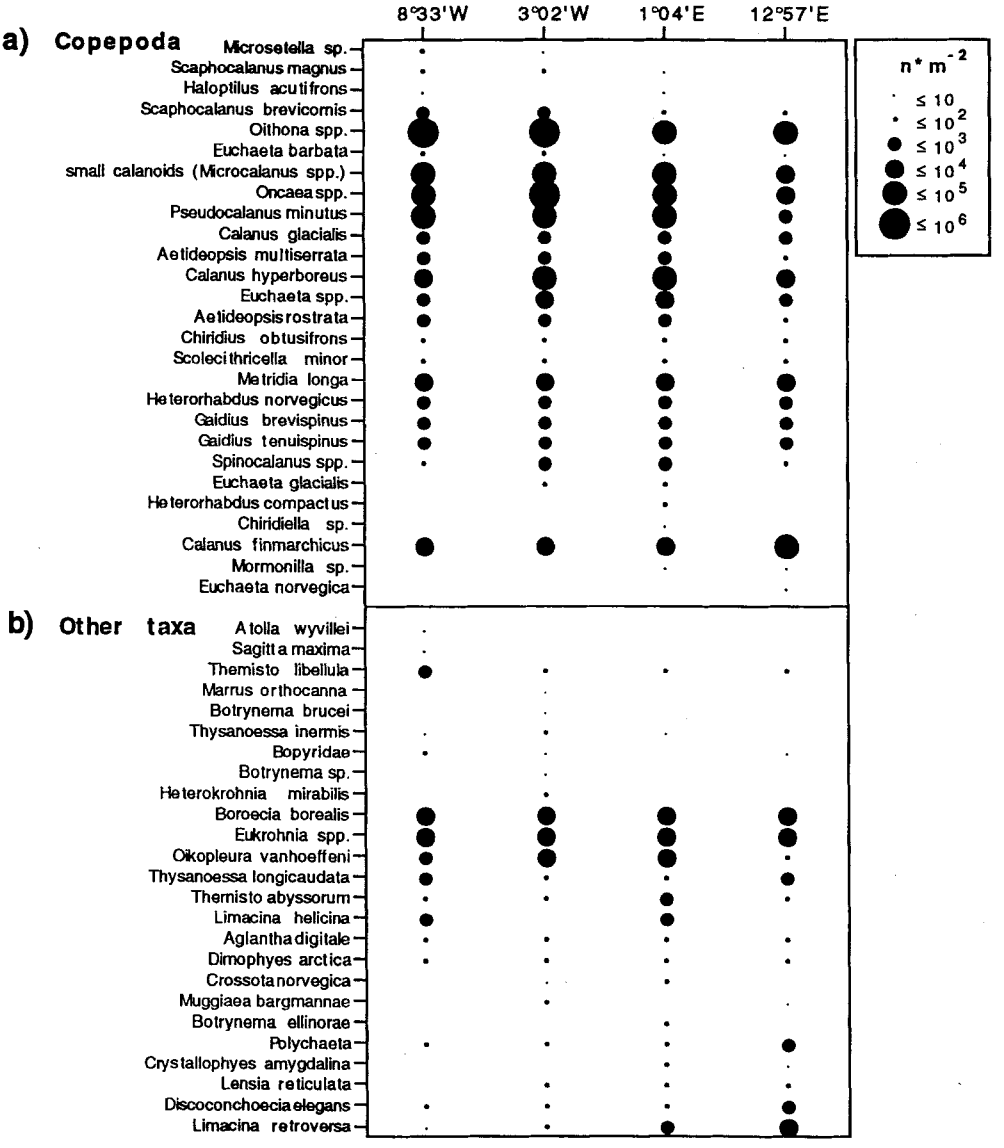

Fig. 4.16: 'Mumm-plot' of species abundances for the regional transect across the Greenland Sea in November 1988, separated for copepods (a) and 'other taxa' (b). Species are ranked according to their zonal center of distribution; species with a westerly distribution are listed above, those with an easterly distribution below.

abundant in the WSC (13°E). This station differs from the gyre stations in generally lower abundances (except for the stated taxa), but no clear zonal pattern is detectable due to the coarse logarithmic scale, the paucity of stations and the ubiquity of the commoner taxa.

The 'Mumm-plot' for the seasonal distribution of copepods is shown in Fig. 4.17a. Taxa with highest occurrences in the dark season are listed in the upper panel, those abounding during the light season at the lower end.

Disregarding the incidental reports of those taxa represented by only single or scattered specimens, virtually no copepods represent the winter type and few, if any, the summer type. The rectangular array of the occurrences rather indicates that all the common copepods are present in the GSG throughout the year. Furthermore, all occur in fairly high numbers, irrespective of season.

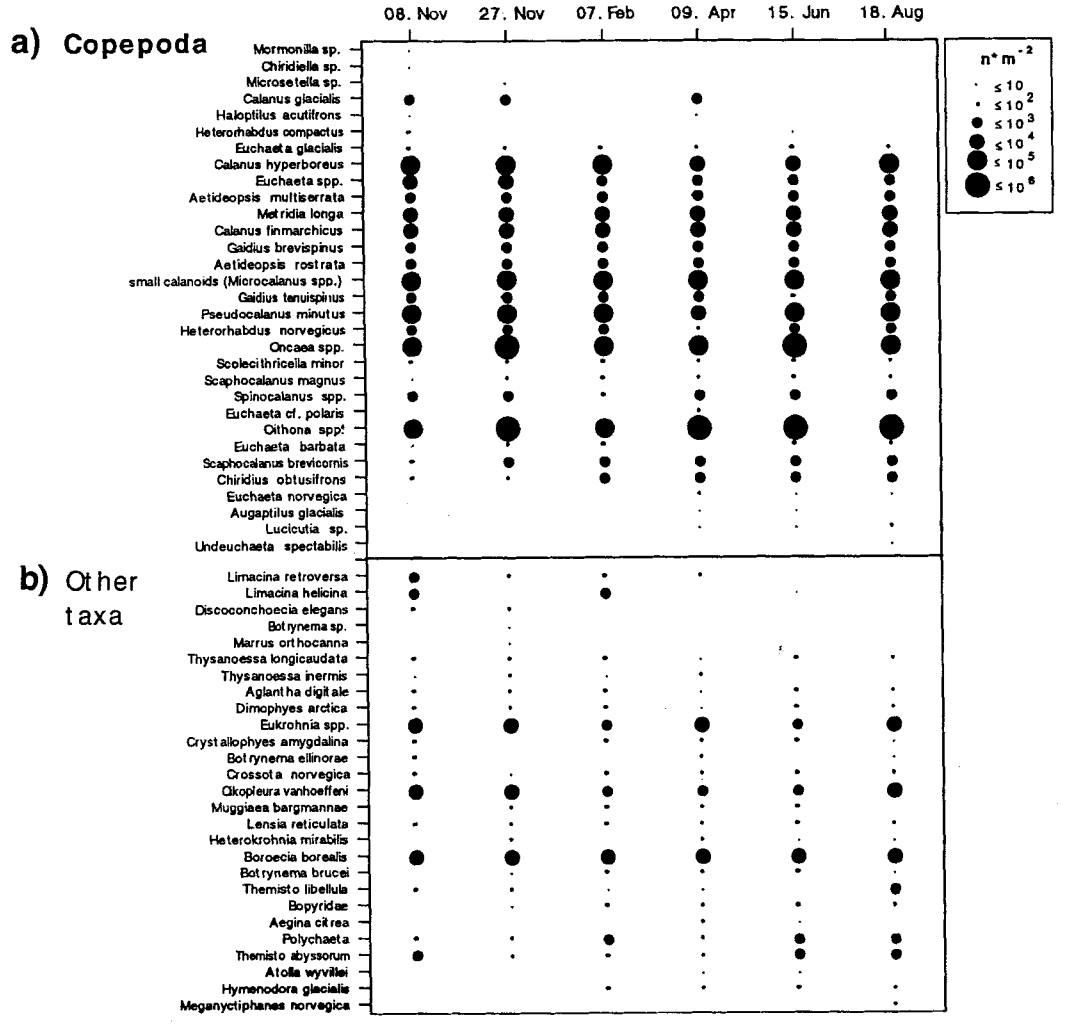

Fig. 4.17: 'Mumm-plot' of species abundances for the seasonal study in the Greenland Sea Gyre, separated for copepods (a) and 'other taxa' (b). Species are ranked according to their seasonal center of distribution; species with highest occurrences in winter are listed above, those with highest occurrences in summer below.

The array takes a more slanted appearance for the other taxa (Fig. 4.17b) and it is noteworthy that some of the species which are common in late fall (*Limacina retroversa, L. helicina, Discoconchoecia elegans*) vanish in summer. while none of the summerly occurring taxa are absent in winter, two incidental macroplankton species notwithstanding. These findings have to be born in mind when discussing advective versus biological causes of population changes in the Greenland Sea Gyre (GSG).

The yearly-averaged vertical distribution of GSG zooplankton is depicted in Fig. 4.18. A clear pattern separates surface from deep dwellers in both, copepods and other taxa. The trapezoidal array of occurrences shown in the plot reveals the interesting observation that the designated 'surface' dwellers do occur throughout the water column down to the

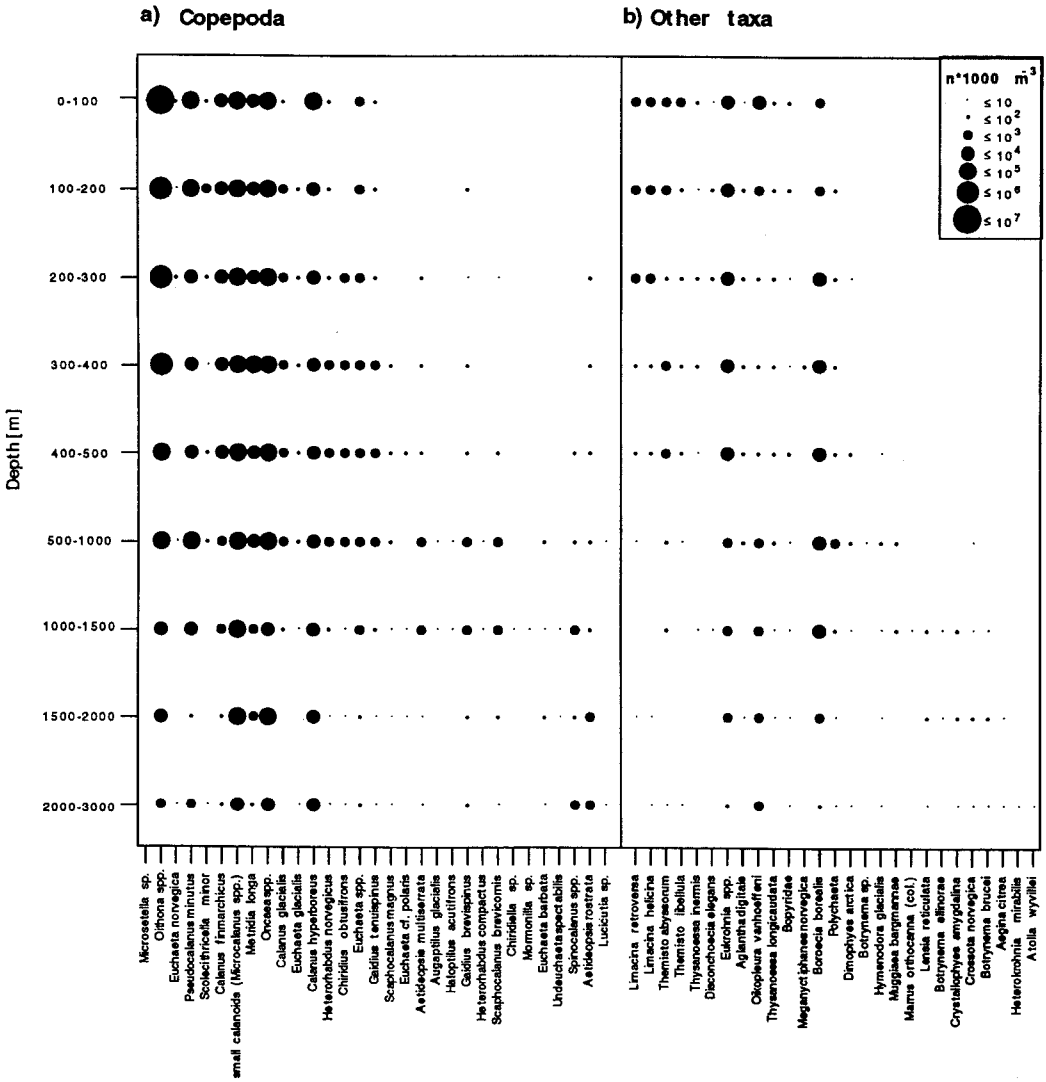

Fig. 4.18: 'Mumm-plot' of species abundances of copepods (a) and 'other taxa' (b) in the nine depth strata. Species are ranked according to their vertical center of distribution; species with a surface-biassed distribution are listed above, those with a deep distribution below.

greatest depths, whereas deep dwellers do not extend into the surface layers. This is most evident for the 'other' taxa, e.g. the hydromedusan and siphonophoran species which occur in low numbers but regularly and exclusively in the bathypelagic range (Fig. 4.18b). Copepods seem to be less restricted in their vertical range. However, a layered distribution of copepods is discernible at intermediate and great depths. Most of the species following this distribution pattern belong to the family Aetideidae. About half of the taxa encountered of both, copepods and 'others', have a very broad vertical range on a yearly basis, extending from the surface to the deep sea. These are also the numerical (*Oithona, Oncaea*) as well as biomass (*Calanus hyperboreus, Eukrohnia hamata, Boroecia borealis*) dominants (cf. Table 4.2)

It will be shown in the following, that many of these species undergo seasonal vertical migrations and abound in much narrower depth ranges on a shorter time scale. Furthermore, it appears that the ranking of the species within this category reflects the range of seasonal migration. This issue will be taken up again in section 4.3 on distribution patterns of selected species.

4.2 Community structure

It was already emerging from the foregoing chapters, that vertical structure appears to be more evident than horizontal structure in the distribution patterns of zooplankton in the Greenland Sea. The ANOSIM permutation test for depth versus time effects on community patterns among samples leads to rejection of H_{01} („no depth effects") at virtually any significance level one cares to nominate (Table 4.4). The observed ρ_{av} is larger than its value in any of the 5000 permutations under H_{01} ($p<0.0002$).

By contrast, the test of the hypothesis H_{02} („no time effects") yields a ρ_{av} which is exceeded by almost half of the simulated values under H_{02} and the null hypothesis cannot be rejected ($p= 0.487$). The test leads to the conclusion that depth is a highly significant factor in shaping the zooplankton community whereas season is not.

Table 4.4: ANOSIM permutation test for differences between time groups (averaged across 9 depth groups) and differences between depth groups (averaged across 6 time groups) in zooplankton samples from the Greenland Sea Gyre. Two-way crossed layout without replication.

Test for difference between	time groups	depth groups
Sample statistic ρ_{av}	-0.006	0.684
Number of permutations	5000	5000
Number of permuted statistics $\geq\rho_{av}$	2432	0
Significance level of ρ_{av}	48.7% (n.s.)	<0.02% (***)

n.s.= not significant, *** highly significant

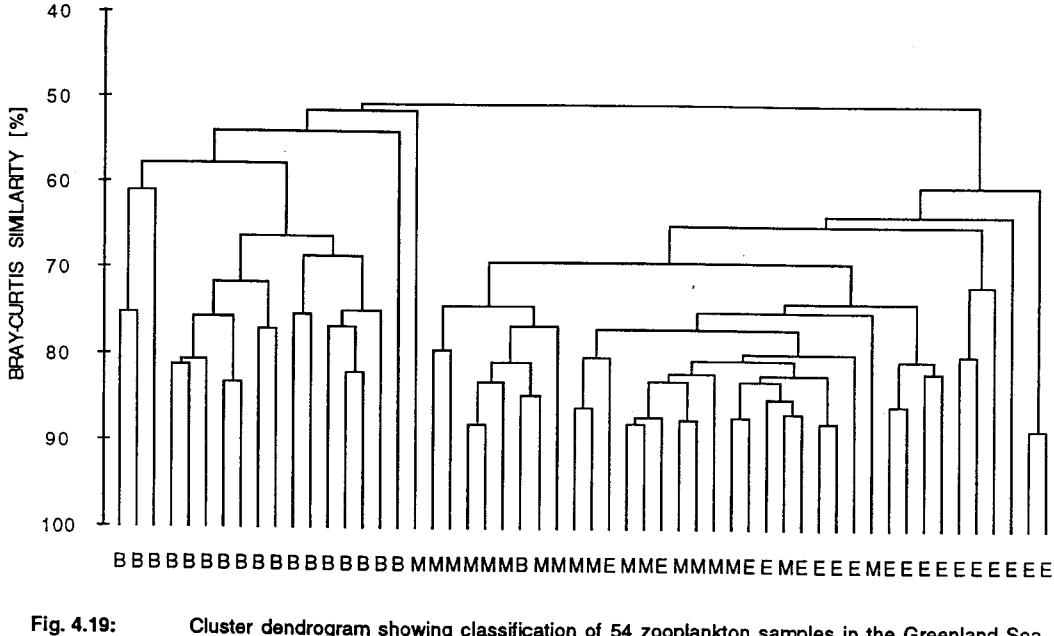

Fig. 4.19: Cluster dendrogram showing classification of 54 zooplankton samples in the Greenland Sea Gyre (fourth-root transformed abundances, Bray-Curtis similarity, group average linking). Samples are labelled according to depth (E= 0-300 m; M= 300-1000 m; B= 1000-3000 m).

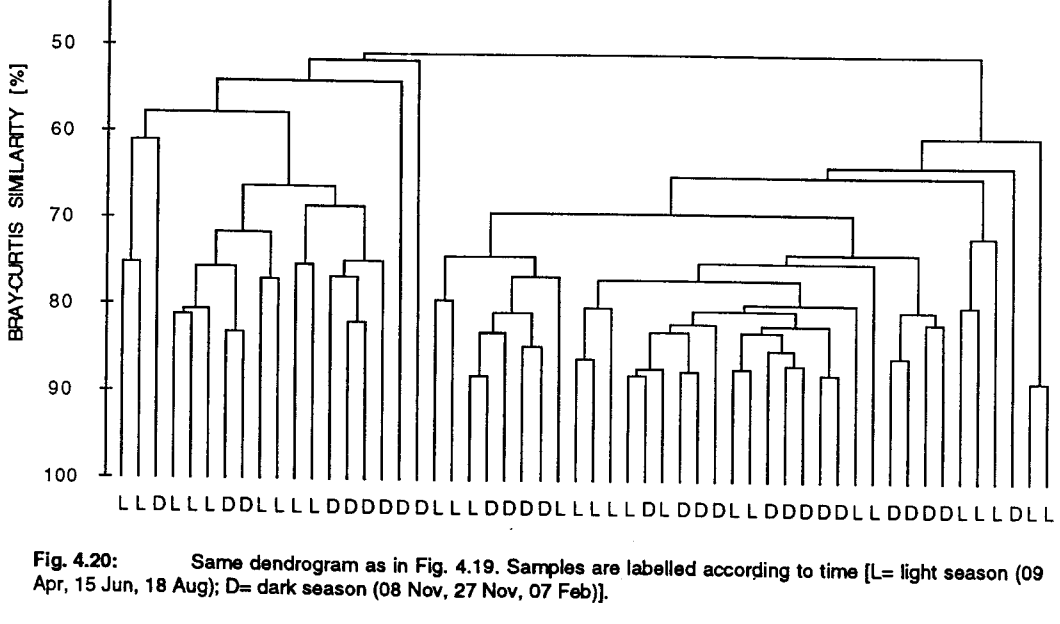

Fig. 4.20: Same dendrogram as in Fig. 4.19. Samples are labelled according to time [L= light season (09 Apr, 15 Jun, 18 Aug); D= dark season (08 Nov, 27 Nov, 07 Feb)].

As expected from the ANOSIM test, subsequent classification analysis results in a clustering of samples according to depth: Epi (E)-, meso (M)- and bathypelagic (B) samples are grouped in conspicuous clusters (Fig. 4.19). Season, by contrast, appears to be irrelevant to the observed grouping of samples (Fig. 4.20).

The same depth dependence is borne out by the MDS ordination yielding a near total separation of bathypelagic from epi- and mesopelagic samples (Fig. 4.21). The separation of epi- and mesopelagic samples is even more evident than in the cluster dendrogram, but the overlap of the E and M labels shows that they are part of a continuum. The isolated E and M samples in the plot, denoted by an asterisk, correspond to the seasonal extremes in total abundance in mid-June (surface layer) and February (400-500 m, cf. Fig. 4.13). The MDS plot with samples labelled according to season bears no structure at all (Fig. 4.22).

Classification and ordination was repeated for the 39 species (Figs. 4.23 and 4.24). The resulting dendrogram reveals six species clusters (Fig. 4.23). Cluster 1 is composed of cnidarians, which all occur exclusively and fairly regularly, but in low numbers in the bathypelagial (cf. Fig. 4.18). Cluster 2 is more heterogeneous in phyletic composition grouping species of regular occurrence in the mesopelagial. The third cluster assembles the biomass and abundance dominants, which all undergo more or less pronounced seasonal vertical migrations. The next two clusters are heterogenous assemblages of meso- and bathypelagic organisms, which is more difficult to interpret. Cluster 6, finally, groups the pteropods *Limacina helicina* and *L. retroversa*, which were shown to have a regionally, seasonally and vertically biassed distribution (Figs. 4.16-18).

The most conspicuous of these clusters, namely 1, 3 and 6 are also easily recognizable assemblages in the MDS plot (Fig. 4.24), and it is not surprising to find the 'predictible' deep dwellers of cluster 1 and the 'unpredictable' surface-biassed pteropods (cluster 6) on opposite sides of the plot. The representatives of cluster 3 project downwards from a diffuse center assemblage, and the array '*Oithona*, *Oncaea*, nauplii, etc.' reads like the 'top

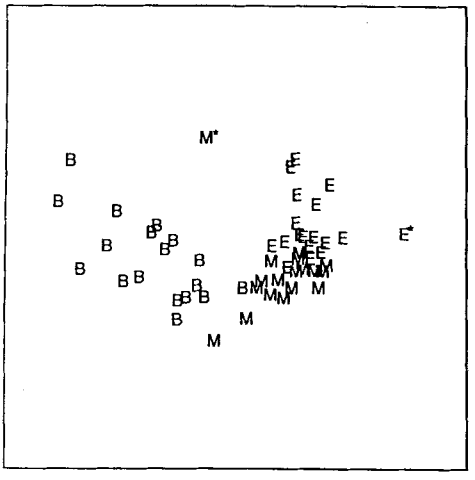

Fig. 4.21: Ordination of 54 zooplankton samples in the Greenland Sea Gyre in 2 dimensions using multi-dimensional scaling on the same similarity matrix as in Fig. 4.19. Axis scales are arbitrary. Asterisks denote the seasonal extremes in total abundance (cf. text). For legend cf. Fig. 4.19.

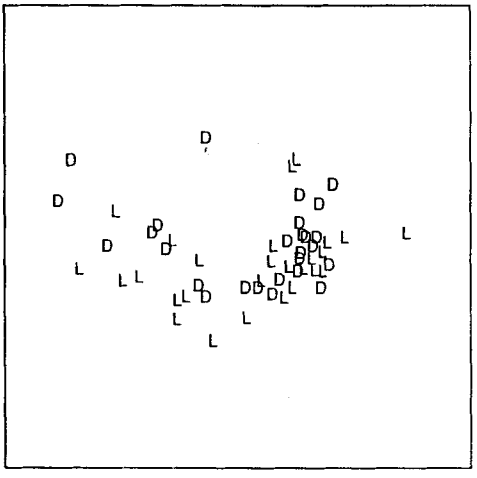

Fig. 4.22: Same MDS plot as in Fig. 4.21. Samples are labelled according to time (cf. Fig. 4.20). Axis scales are arbitrary.

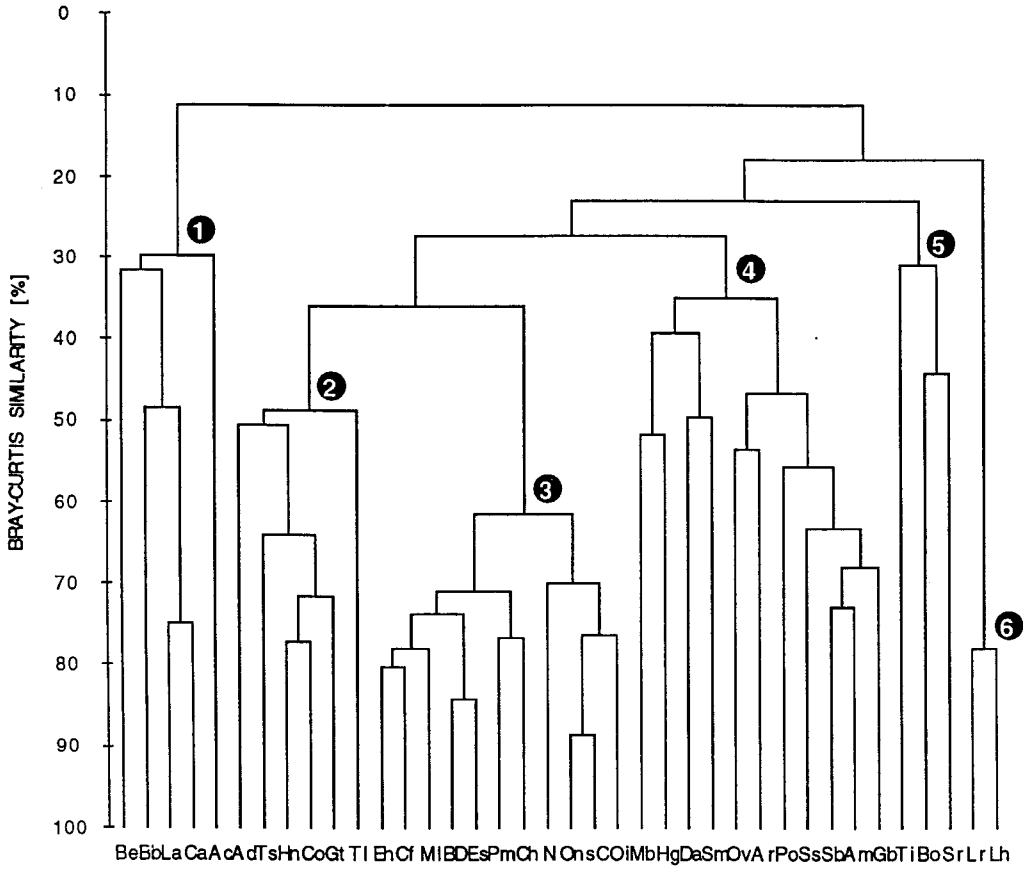

Fig. 4.23: Cluster dendrogram showing classification of 39 zooplankton taxa in the Greenland Sea Gyre (fourth-root transformed abundances, Bray-Curtis similarity, group average linking). Clusters are numbered 1 to 6.

(Be=*Botrynema ellinorae*, Bb= *Botrynema brucei*, La= *Lensia reticulata*, Ca= *Crystallophyes amygdalina*, Ac= *Aegina citrea*, Ad= *Aglantha digitale*, Ts= *Themisto* sp., Hn= *Heterorhabdus norvegicus*, Co= *Chiridius obtusifrons*, Gt= *Gaidius tenuispinus*, Tl= *Thysanoessa longicaudata*, Eh= *Eukrohnia* spp., Cf= *Calanus finmarchicus*, Ml= *Metridia longa*, BD= *Boroecia/Discoconchoecia*, Es= *Euchaeta* spp., Pm= *Pseudocalanus minutus*, Ch= *Calanus hyperboreus*, N= nauplii, On= *Oncaea* spp., sC= small calanoids, Oi= *Oithona* sp., Mb= *Muggiaea bargmannae*, Hg= *Hymenodora glacialis*, Da= *Dimophyes arctica*, Sm= *Scaphocalanus magnus*, Ov= *Oikopleura vanhoeffeni*, Ar= *Aetideopsis rostrata*, Po= Polychaeta, Ss= *Spinocalanus* spp., Sb= *Scaphocalanus brevicornis*, Am= *Aetideopsis multiserrata*, Gb= *Gaidius brevispinus*, Ti= *Thysanoessa inermis*, Bo= Bopyridae, Sr= *Scolecithricella minor*, Lr= *Limacina retroversa*, Lh= *Limacina helicina*

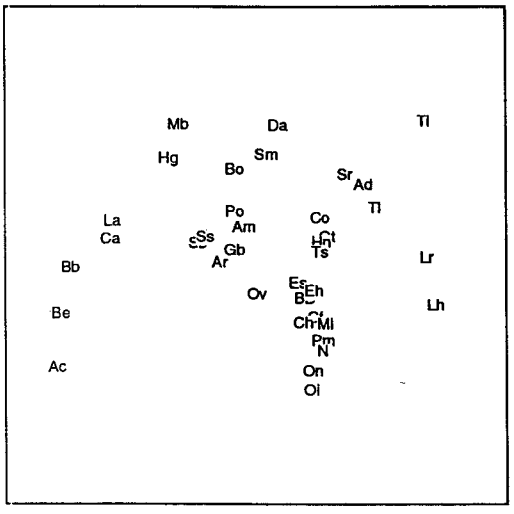

Fig. 4.24: Ordination of 39 zooplankton taxa in the Greenland Sea Gyre in 2 dimensions using multidimensional scaling on the same similarity matrix as Fig. 4.23. Axis scales are arbitrary. For legend cf. Fig. 23

ten' list of abundances (Table 4.2). In the center of the plot we find species of the meso- and bathypelagic copepod family Aetideidae. It is noteworthy that their alignment matches their vertical centers of distribution, as will be shown later, with the mesopelagic *Chiridius obtusifrons* and *Gaidius tenuispinus* to the right and the truly bathypelagic *G. brevispinus* and *Aetideopsis rostrata* to the left of the array.

4.3 Selected species

This section highlights the distribution and quantitative composition of those taxa which were shown to be dominant or to represent a particular distribution type. Where appropriate, the chapters are followed by short interpretations of the results (in italics) to set the stage for the discussion of the life history of these groups in the Greenland Sea (cf. chapter 5.4).

Numerical dominants (Cyclopoida and small Calanoida)

Oithona

Oithona is by far the most abundant taxon encountered during this study, contributing to about half of total zooplankton numbers (Table 4.2). But due to its relatively small size, it constitutes only about 2% and 4% of total biomass, averaged across the regional transect in late fall, and across all seasons in the Greenland Sea Gyre (GSG), respectively.

Figure 4.25 reveals marked regional and seasonal differences of abundance and length composition across the Greenland Sea, and within the GSG, respectively.

The lowest numbers of individuals are found at 13°E ($22*10^3$ $n*m^{-2}$) in late fall, while about seven-fold higher values are recorded to the west of the Arctic Front (Fig. 4.25a). These abundance differences are compounded by conspicuous changes in the length distribution between the Atlantic and the arctic stations. The former displays a clear bimodal distribution with modal classes of +0.6 and +1.2 mm total length[4], while the larger-sized mode is entirely absent in the gyre, not only in late fall, but throughout the investigation period (Figs. 4.25a and b, note the scale difference between a and b). Microscopic identification confirms the presence of two species at 13°E but of only one further west. *Oithona similis* (0.8 mm total length) occurs throughout the Greenland Sea, while the larger *O. atlantica* (up to 1.4 mm total length) is confined to 13°E.

Additional regional variability occurs within the lower-sized mode: The length frequency changes from a broad-range left[5]-skewed distribution dominated by large +0.8 mm animals at the western station towards a narrow-range right-skewed distribution dominated by smaller +0.6 mm animals at the eastern station. The center station at 1°E displays a more or less symmetrical distribution around a plateau-like mode of constant frequencies between 0.6 and 0.9 mm. It is very likely that this pattern arises from overlapping 'eastern' and 'western' distribution types described above.

[4] + denotes the left bin edge of a 0.05 mm size class

[5] left and right refers to the small and large size ends, respectively

Acknowledgements

I would like to thank Prof. G. Hempel for supervising this dissertation, for valuable suggestions and for the swif critical revision of the thesis.
This work would not be ossible without the initiative and encouragement of Dr. H.-J. Hirche and the excellent cooperation with him and other co-workers of the Greenland Sea Project, namely Dr. R. Weigmann-Haass, T. Scherzinger, Dr. W. Hagen, J. Wegner and Dr. D. Quadfasel, who made available their samples and data to this study.
Special thanks to Dr. W. Hagen for competent advice throughout this investigation and painstaking revision of the manuscript. Dr. R. Gradinger reviewed an earlier, and Prof. M. Spindler the final draft of the thesis.
Dr. N. Mumm introduced me to Arctic zooplankton, Drs. F. Pagès, K. Hülsemann and S. Kwasniewski helped in solving taxonomic problems.
Dr. D. Piepenburg gave statistical advice and Dr. K.R. Clarke provided the ANOSIM program.
Thanks to all members of the Institut für Polarökologie for a truly exceptional working environment.
Finally, I would like to thank my family for their loving support and patience.

This work was financed by a fellowship from the State of Schleswig-Holstein and by the Deutsche Forschungsgemeinschaft (DFG) through the Sonderforschungsbereich (SFB) 313 of Kiel University.

APPENDIX 1.1

Mean individual dry weights (DW_i) used in the biomass calculations with references to source of data

Taxon	Stage	DW_i [mg]	s.d.	Pres.	Season	Region	Reference
Calanus finmarchicus	CVI m	†0.28	-	-	-	-	-
	CVI f	0.327	0.076	1,2	4,5	2,3,4,5,6	2,5,7,8
	CV	0.274	0.098	1,2	4,5	2,3,4,6	2,5,8,
	CIV	*0.128	-	-	2	5	3
	CIII	*0.046	-	-	2	5	3
Calanus glacialis	CVI m	0.752	0.179	3	2,3,4	1	4,9
	CVI f	0.890	0.235	2,3	2,3,4,5	1,2,5	4,5,6,7,9
	CV	0.778	0.307	2,3	2,3,4,5	1,2,3	4,5,9
	CIV	0.169	0.064	2,3	2,3,4,5	1,3	4,5,9
	CIII	0.043	0.014	3	2,3,4,5	1	4,9
Calanus hyperboreus	CVI m	1.254	0.250	3	2	1	4,9
	CVI f	2.350	0.689	2	2,3,4	3	5,6
	CV	1.021	0.452	2	2,3,4	3	5,6
	CIV	0.206	0.017	2	2,4	3	5,6
	CIII	0.056	0.005	2	4	3	5
Metridia longa	CVI m	0.137	0.037	1,2,3	2,3,4,5	1,3,6	2,4,5,9
	CVI f	0.287	0.045	2	3,4	3	5
	CV	0.120	0.036	2,3	2,3,4,5	1,3	4,5,9
	CIV	0.034	0.006	2,3	2,3,4,5	1,4	4,5,9
Euchaeta barbata	CVI m	†2.973	-	2	4	4	5
	CVI f	9.056	0.255	2	4	3,4	5
Euchaeta glacialis	CVI m	3.348	-	2	4	1	5
	CVI f	5.907	1.129	2	3,4	1,2,3	5
Euchaeta norvegica	CVI m	1.789	0.185	1,2	1-5	1,6	1,5,12
	CVI f	4.672	0.756	1,2	1-5	2,6	1,5,12
Euchaeta spp.	CV	1.681	0.882	2	4	1,4	5
	CIV	0.377	0.009	2	4	4	5
	CIII	*0.121	0.017	2	5	3	13
	CII	*0.048	0.011	2	5	3	13
	CI	*0.038	0.010	2	5	3	13
Scaphocalanus magnus	CVI m	†0.635	0.062	2	4	1	5
	CVI f	0.722	0.023	2	4	1	5
Scaphocalanus spp.	-	0.035	0.004	2	2	7	10
Scolecithricella minor	-	0.024	0.004	2	2	7	10
Pseudocalanus minutus	-	*0.023	0.009	2	5	3	13
Microcalanus spp.	-	*0.007	0.004	2	5	3	13
Spinocalanus spp.	-	0.013	0.004	2	2	7	10
Oithona spp.	-	0.003	0	1,3	4,5	1,6	2,11
Oncaea spp.	-	*0.002	<0.001	2	5	3	13
nauplii	-	†0.001	-	-	-	-	-
Bopyridae	-	*0.030	-	2	5	3	13
Meganyctiphanes norvegica	-	65	35	2	3,4	1,2,4	5
Thysanoessa inermis	-	33	17	2	3,4	1,4	5
Thysanoessa longicaudata	-	4	1	2	3,4	1,3,4	5
Hymenodora glacialis	-	41	32	2	4	1,3,4	5
Polychaeta	-	*0.062	-	2	5	3	13
Limacina spp.	-	0.343	-	2	4	4	5
Oikopleura vanhoeffeni	-	‡0.2	-	3	4	1	11

APPENDIX 1.1 (continued)

Taxon	Stage	DW_i [mg]	s.d.	Pres.	Season	Region	Reference
Crystallophyes amygdalina	-	†0.8	-	-	-	-	-
Dimophyes arctica	-	‡0.8	-	3	4	1	11
Muggiaea bargmannae	-	†0.8	-	-	-	-	-
Aegina citrea	-	1.9	1.0	3	1,3	3	13
Aglantha digitale	-	2.9	1.2	3	1,3	3	13
Botrynema spp.	-	6	4	3	1,3	3	13

Abbreviations: s.d.= standard deviation (or range), Pres.= Preservation method

Number codes:
•Pres. [1= fresh, 2= frozen, 3= formaline]
•Season [1= winter, 2= spring, 3=early summer, 4= summer, 5= fall]
•Region [1= Arctic/East Greenland shelf, 2= Fram Strait, 3= Greenland Sea Gyre, 4= West Spitsbergen Current/Norwegian Sea, 5= Barents Sea, 6= Kosterfjorden, 7= Southern Ocean]
•Reference [1= Båmstedt 1981, 2= Båmstedt et al. 1990, 3= Båmstedt et al. 1991, 4= Conover and Huntley 1991, 5= Hagen (unpubl.), 6= Hirche et al. 1994, 7= Ikeda and Skjoldal 1989, 8= Kattner et al. 1989, 9= Kosobokova 1980, 10= Mizdalski 1988, 11= Mumm 1991, 12= Norrbin and Båmstedt 1984, 13= Richter (unpubl.)]

Symbols: *= converted from carbon (C), ‡= converted from ash free dry weight (AFDW), assuming C:DW=0.5 and AFDW:DW= 0.9 (Båmstedt 1986). AFDW:DW= 0.4 was used for Siphonophora (Clarke et al. 1992). †= inferred from length

APPENDIX 1.2

Dry weight-length relationships used in biomass calculations and references to source of data

Taxon	a	b	r^2	c	Pres.	Season	Region	Reference
Aetideopsis spp.	*0.005	4.659	0.79	p	frozen	fall	GSG	3
Chiridius/Gaidius spp.	†0.010	3.412	0.90	"	formaline	summer	AO	2
Heterorhabdus norvegicus	†0.003	4.716	0.99	"	"	"	"	2
Boroecia/Discoconchoecia sp.	‡0.033	2.370	0.95	"	formaline	summer	AO	2
Themisto spp.	¥0.009	2.407	0.94	"	"	"	"	2
Eukrohnia spp.	0.041	0.165	0.95	e	"	fall	GSG	1
Crossota norvegica	0.322	0.191	0.97	"	"	winter, summer	"	3

Dry weight (DW) in mg, length (L) in mm of cephalothorax (Copepoda) or longest dimension of animal. Coefficients [a, b] and coefficient of determination [r^2] are given for power ($DW= aL^b$) or exponential regression ($DW= ae^{bL}$). Curve fit [c] is indicated (e= exponential, p= power fit), as is the preservation method [Pres.]

Abbreviations: AO= Arctic Ocean, GSG= Greenland Sea Gyre

References: 1= Hirche (unpubl.), 2= Mumm 1991, 3= Richter (unpubl.)

Symbols: *= converted from carbon (C), †= converted from ash-free dry weight (AFDW), assuming C:DW=0.5 and AFDW:DW=0.9 (Båmstedt 1986), ‡= converted from AFDW, assuming AFDW:DW=0.7 [cf. Mizdalski (1988) for *Conchoecia*], ¥= converted from AFDW, assuming AFDW:DW=0.8 [cf. Båmstedt (1981) for *Parathemisto*]